

Dynamical Contributions to Enzyme Catalysis: Critical Tests of A Popular Hypothesis

Mats H. M. Olsson,^{*,†} William W. Parson,^{*,‡} and Arieh Warshel^{*,†}

Department of Chemistry, University of Southern California, 3620 McClintock Avenue, Los Angeles, California 90089-1062, and Department of Biochemistry, University of Washington, Box 357350, Seattle, Washington 98195-7350

Received September 8, 2004

Contents

1. Introduction	1737
2. Defining Catalytic Effects	1738
3. Evaluating Activation Free Energies	1739
4. The Rate Constant	1740
5. The Transmission Coefficient	1740
6. The Autocorrelation Function of the Energy Gap Is Similar in Enzymes and Solution	1741
7. The Relaxation Dynamics of the Effective Solute and Solvent Coordinates Are Similar in Enzymes and Solution	1742
8. Nonequilibrium Solvation Does Not Contribute a Dynamical Effect	1744
9. The Frequencies of Catalytically Important Vibrational Modes in Enzymes Are Similar to Those in Solution	1746
10. Tunneling and Other Nuclear Quantum Mechanical Effects Do Not Contribute to Catalysis in a Major Way	1747
11. Concerted Motions in an Enzyme Usually Do Not Make Dynamical Contributions to Catalysis	1751
12. Other Proposals for How Enzymes Work	1753
13. Conclusions	1754
14. Acknowledgment	1754
15. References	1754

1. Introduction

Enzymes play fundamental roles in almost all life processes. They accelerate a great variety of metabolic reactions and they control signaling, energy transduction, and transcription and translation of genetic information. Their ability to catalyze reactions by many orders of magnitude allows cells to carry out reactions that otherwise would not occur on biologically useful time scales. There is, therefore, broad interest in understanding the origin of this catalytic power on a molecular level.

Many proposals have been put forward to rationalize the catalytic power of enzymes (see Villà and Warshel¹ for a partial list). As discussed elsewhere,^{1,2} some of these proposals are problematic or difficult to analyze quantitatively. Although mutation experiments have been extremely

useful for identifying catalytic factors,³ they cannot identify the mechanism of catalysis uniquely. Computer simulation studies generally have favored the view that the most important catalytic factor is stabilization of the transition state (TS) by electrostatic preorganization of the enzyme active site and that other effects usually are relatively small.^{1,2,4,5} However, it is important to continue to entertain alternatives to electrostatic preorganization. In particular, many investigators have asked whether “dynamical effects” play a significant role in enzyme catalysis.

By a dynamical effect, we mean that the enzyme has evolved to optimize a particular vibrational mode for moving the system to the TS, or for converting a system at the TS to the product state. One of the clearest explanations of this possibility has been given by Karplus and McCammon,⁶ who stated,

Fluctuations could play an essential role in determining the effective barriers for the catalyzed reactions. If the substrate is relatively tightly bound, local fluctuation in the enzyme could couple to the substrate in such a way as to significantly reduce the barriers. If such coupling effects exist, specific structures could have developed through evolutionary pressure to introduce directionality and enhance the required fluctuations....

Energy released locally in substrate binding may be utilized directly for catalyzing its reaction, perhaps by introducing certain fluctuations.

The essence of the proposal is that the motions of the reacting groups are different in enzymatic and nonenzymatic reactions and, specifically, that the motions in the enzyme are more directional than the random thermal fluctuations that establish a Boltzmann equilibrium between the reactants and the TS for a reaction in solution. Thus, dynamical effects must be at work if a system at the TS has a higher probability of decaying to products in the enzyme than it does for the same reaction in solution. Dynamical effects also would be implicated if the catalysis depends on coherent vibrations that do not obey a Boltzmann distribution. Conversely, if we can account for the enzymatic rate constant simply by using a Monte Carlo procedure to evaluate the activation free energy, then the catalysis must not involve dynamical effects. Dynamical effects also might arise if reactions in solution and in enzymes involve qualitatively different mixtures of solute and solvent coordinates or if the solvent coordinates are much more (or less) frozen in a protein than in solution.⁷

The idea that dynamical effects play a major role in enzyme catalysis dates back at least 25 years.^{6,8–10} It has

* Corresponding authors. M.H.M.O.: e-mail molsson@usc.edu; phone 213 740 7671; fax 213 740 2701. W.W.P.: e-mail parsonb@u.washington.edu; phone 206 543 1743; fax 206 685 1792. A.W.: e-mail warshel@usc.edu; phone 213 740 1441; fax 213 740 2701.

[†] University of Southern California.

[‡] University of Washington.



Mats Olsson was born in Malmo (Sweden) and received his M.Sc. and Ph.D. in theoretical chemistry at Lund University working with B. O. Roos and U. Ryde. In 2000, he joined Dr. Arieh Warshel's research group for postdoctoral studies, where he is currently working as a research associate. His current research interests are focused on modeling electron and proton transfer.



William Parson is Professor of Biochemistry and Adjunct Professor of Chemistry at the University of Washington. He received his undergraduate training at Harvard, Ph.D. in Biochemistry at Western Reserve University, and postdoctoral training in biophysics at the University of Pennsylvania. He was Associate Editor of *Biochemistry* from 1969 to 2000 and recipient of the Repligen Award in Biological Chemistry in 1991. His main research interests have been electron and energy transfer in photosynthetic bacteria, which he has studied by fast spectroscopic techniques and computer modeling. Current interests include structural and functional studies of the enzyme catechol-*O*-methyltransferase. In addition to science, he enjoys music, hiking in the Cascades and Olympic ranges, and trekking in remote parts of the world.

gained momentum since the mid-1990s and continues to attract considerable attention.^{7,11–27} Although we^{1,5,28–30} and others^{31,32} have challenged the significance of dynamical effects, the idea clearly has durable appeal.

This review examines whether dynamical effects contribute significantly to enzyme catalysis. Our main concern will be the use of computer simulations to address this question quantitatively.

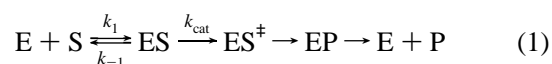
In examination of dynamical proposals, there is a tendency to describe different views of the catalytic role of enzyme dynamics as *semantic* issues. However, the key issues concern the catalytic mechanisms that have been proposed and not what names were used to describe such proposals. Since we believe that the fundamental points at issue rise considerably above the level of semantics, we will focus here on the specific mechanisms that actually have been proposed.



Arieh Warshel is a professor of Chemistry and Biochemistry at the University of Southern California. He was born in Kibutz Sdhe Nahum, Israel, and received his B.Sc. in 1966 from the Technion Institute in Israel. He then earned his M.Sc. in 1967 and Ph.D. in 1969 from the Weizmann Institute. His Ph.D. with Shneior Lifson and collaboration with Mike Levitt is the basis of many current molecular simulation programs. Between 1970 and 1976, he held a postdoctoral position at Harvard University, returned to the Weizmann Institute, and was an EMBO fellow at the MRC in Cambridge. In 1976, he joined the Department of Chemistry at the University of Southern California. He has pioneered computer-modeling approaches for studies of protein functions. These include the development of consistent treatments of electrostatic energies in proteins, the development of hybrid quantum mechanical/molecular mechanics (QM/MM) approaches for studies of enzymatic reactions, the introduction of molecular dynamics simulations to studies of biological processes, and the introduction of microscopic evaluation of thermodynamics cycles in biological systems. Warshel's group focuses on simulations of structure–function correlation of biological systems. Professor Warshel is the author of *Computer Modeling of Chemical Reactions in Enzymes and Solutions*, published in 1991, he received the 1993 award of the International Society of Quantum Biology and Pharmacology, and he is a fellow of the Biophysical Society and a recipient of the 2003 Tolman Award. The nonscientific interests of Dr. Warshel include indiscriminately watching different television programs.

2. Defining Catalytic Effects

Consider the generic enzymatic reaction



where E, S, and P are the enzyme, substrate, and product, respectively, and ES, EP, and ES[‡] are the enzyme–substrate complex, enzyme–product complex, and transition state. As was shown convincingly by Wolfenden and co-workers,³³ many enzymes appear to have evolved to optimize k_{cat}/K_M , where $K_M = (k_{-1} + k_{\text{cat}})/k_1$. This optimization can involve maximizing k_{cat} , minimizing K_M , or both. The present article considers k_{cat} .

To evaluate enzyme catalysis quantitatively, we first must ask “catalysis relative to what?” The most obvious reference is the uncatalyzed reaction in water (see Figure 1). Since the mechanism of the reaction can be different in water than in the enzyme, changes in the mechanism must be considered in addition to the effects of altering the environment. But differences in mechanism such as using a general base instead of water as a base can be classified as “chemical effects”, and such effects are well understood. Our reference, then, should be a reaction that occurs by the same mechanism in water, so that the question becomes how the structured environment in the enzyme accelerates the reaction relative to the same process in a solvent cage.²

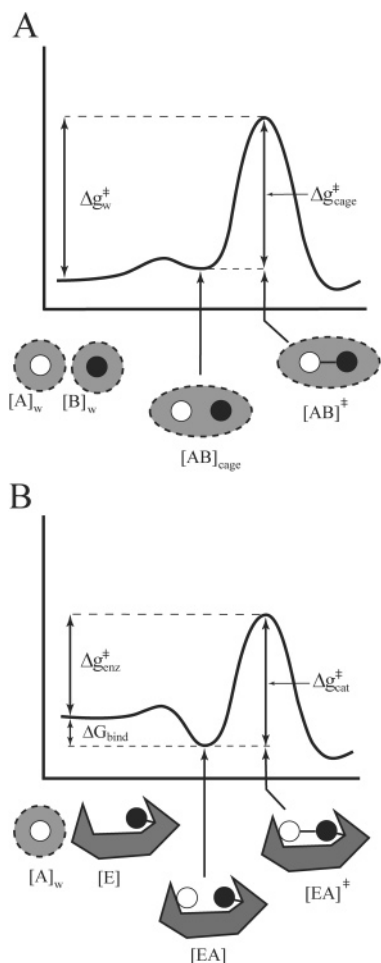
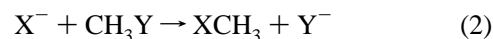


Figure 1. Free energy profiles along the paths of a reaction in solution (A) and in an enzyme (B). In solution, the reactants (filled and empty circles in the drawings at the bottom) must move from individual solvent shells to a single solvent cage. The activation free energy of interest ($\Delta g_{\text{cage}}^{\ddagger}$) is the free energy required to form the transition state in the solvent cage. The comparable quantity in an enzyme ($\Delta g_{\text{cat}}^{\ddagger}$) is the free energy required to form the transition state from the bound substrates.

3. Evaluating Activation Free Energies

To examine catalytic effects in enzymes, we need quantitative methods for calculating the rate constant of a reaction given the structure of the enzyme. Any such method requires evaluating the potential energy surface that connects the reactant and product states and finding the activation free energy for reaching the TS. Combined quantum mechanical/molecular mechanics (QM/MM) methods provide a generic way of obtaining potential surfaces and, in principle, activation free energies of chemical processes in enzymes. This approach, introduced by Warshel and Levitt in 1976,³⁴ has gained popularity in recent years and has been used in a variety of forms.^{2,35} However, implementation of rigorous ab initio QM/MM approaches in quantitative calculations of activation free energies is still extremely challenging.^{2,36–38} The somewhat less rigorous empirical valence bond (EVB) method^{5,39} provides what is probably the most effective available way of quantifying catalytic effects in general and dynamical contributions in particular. The EVB method is a QM/MM approach that begins with resonance states (or more precisely, diabatic states) corresponding to classical valence-bond structures. These basis states are mixed to describe the reactant intermediate states.

As an example, for a S_N2 reaction of the form



one can use diabatic states of the forms

$$\begin{aligned} \phi_1 &= X^- \text{CH}_3 - Y \\ \phi_2 &= X - \text{CH}_3 \quad Y^- \end{aligned} \quad (3)$$

The potential energies of these states (H_{11} and H_{22}) and the mixing term (H_{12}) are represented by the Hamiltonian matrix elements

$$H_{ii} = \epsilon_i = \alpha_{\text{gas}}^i + U_{\text{intra}}^i(\mathbf{R}, \mathbf{Q}) + U_{\text{inter}}^i(\mathbf{R}, \mathbf{Q}, \mathbf{r}, \mathbf{q}) + U_{\text{solvent}}^i(\mathbf{r}, \mathbf{q}) \quad (4a)$$

$$H_{ij} = A \exp(-a|\Delta R'|) \quad (4b)$$

Here \mathbf{R} and \mathbf{Q} represent the atomic coordinates and charges, respectively, of the reactants or products (“solute”) in the diabatic states, and \mathbf{r} and \mathbf{q} are the coordinates and charges of the surrounding water or protein (“solvent”). α_{gas}^i is the energy of the i th diabatic state in the gas phase, where all the fragments are taken to be at infinity; $U_{\text{intra}}^i(\mathbf{R}, \mathbf{Q})$ is the intramolecular potential of the solute system (relative to its minimum) in this state; $U_{\text{inter}}^i(\mathbf{R}, \mathbf{Q}, \mathbf{r}, \mathbf{q})$ represents the interaction between the solute atoms and the surrounding solvent atoms; $U_{\text{solvent}}^i(\mathbf{r}, \mathbf{q})$ represents the potential energy of the solvent.

The ϵ_i given by eq 4a form the diagonal elements (H_{ii}) of the EVB Hamiltonian (\mathbf{H}_{EVB}). The off-diagonal elements of the Hamiltonian (H_{ij}) either are assumed to be constant or are represented by exponential functions of the distances between the reacting atoms. In the present case we express H_{ij} as a function of the difference between the X–C and C–Y bond lengths ($\Delta R'$ in eq 4b), using parameters (A and a) that are adjusted to fit either quantum calculations or experiment. The H_{ij} parameters are assumed to be the same in the gas phase, in solution, and in the protein. The adiabatic ground-state energy (E_g) and the corresponding eigenvector (\mathbf{C}_g) are obtained by solving the secular equation

$$\mathbf{H}_{\text{EVB}} \mathbf{C}_g = E_g \mathbf{C}_g \quad (5)$$

To express the adiabatic energy surface of the solute–solvent system, it is useful to define a generalized reaction coordinate as the energy gap between the diabatic reactant and product EVB states:

$$x = \Delta \epsilon_{1,2} = \epsilon_2 - \epsilon_1 \quad (6)$$

This coordinate can be divided into a solute coordinate, R , for internal bonds of the reacting EVB structures and a solvent coordinate, S , for interactions of the solute with the solvent. “Solvent” here is used in a general sense to refer to the surroundings of the reacting atoms in either the enzyme or solution. The solvent coordinate is proportional to the difference between the contributions to ϵ_i from electrostatic interactions involving the solvent in the product and reactant states, $\Delta \epsilon_{\text{el}}$ (see Hwang et al.⁴⁰ and section 7):

$$S \propto \Delta \epsilon_{\text{el}} = \epsilon_{\text{el},2} - \epsilon_{\text{el},1} \quad (7)$$

Comparisons of the solvent coordinates in enzyme reactions

with those of reference reactions in solution will be discussed in section 7.

The simplicity of the EVB formulation makes it relatively straightforward to obtain analytical derivatives of the potential surface by using the Hellmann–Feynman theorem for eq 5, and thus to sample the EVB energy surface by molecular-dynamics (MD) simulations. In principle, running MD trajectories on the EVB surface of the reactant state can provide the free energy function (Δg) that is needed to calculate the activation free energy (Δg^\ddagger). However, since trajectories on the reactant surface will reach the TS only rarely, it usually is necessary to run trajectories on a series of potential surfaces (“mapping” potentials) that drive the system adiabatically from the reactant to the product state.⁴¹ In the simple case of two diabatic states such as those of eq 3, the mapping potential (ϵ_m) can be written as a linear combination of the reactant and product potentials, ϵ_1 and ϵ_2 :

$$\epsilon_m = (1 - \lambda_m)\epsilon_1 + \lambda_m\epsilon_2 \quad (8)$$

where λ_m changes from 0 to 1 in $n + 1$ fixed steps ($\lambda_m = 0/n, 1/n, 2/n, \dots, n/n$).

The free energy ΔG_m associated with changing λ from 0 to m/n can be evaluated by a free energy perturbation (FEP) procedure. The free energy functional that corresponds to the adiabatic ground-state surface, E_g , then is obtained by the FEP–umbrella sampling (FEP–US) method,^{5,42} which can be written as

$$\Delta g(x') = \Delta G_m - \beta^{-1} \ln \langle \delta(x - x') \exp\{-\beta[E_g(x) - \epsilon_m(x)]\} \rangle_m \quad (9)$$

In this expression, ϵ_m is the mapping potential that keeps the reaction coordinate x in the region of x' , $\langle \dots \rangle_m$ denotes an average over an MD trajectory on this potential, $\beta = (k_B T)^{-1}$, k_B is the Boltzmann constant, and T is the temperature. If the changes in ϵ_m are sufficiently gradual, the free energy functional $\Delta g(x')$ obtained with several values of m overlap over a range of x' , and patching together the full set of $\Delta g(x')$ gives a complete free energy curve for the reaction.

The FEP–US approach also can be used to obtain the free energy functionals of the individual diabatic states. For example, the free energy of the reactant state (Δg_1) is

$$\Delta g_1(x') = \Delta G_m - \beta^{-1} \ln \langle \delta(x - x') \exp\{-\beta[\epsilon_1(x) - \epsilon_m(x)]\} \rangle_m \quad (10)$$

The diabatic free energy profiles of the reactant and product states represent microscopic equivalents of the Marcus parabolas in electron-transfer theory.^{43,44}

The natural picture of intersecting electronic states provided by the EVB treatment is particularly useful for exploring environmental effects on chemical reactions in condensed phases.⁴² The ground-state charge distribution of the reacting species (solute) polarizes the surroundings (solvent), and the charges of each resonance structure of the solute then interact with the polarized solvent.⁵ This coupling enables the EVB model to capture the effect of the solvent on the quantum mechanical mixing of different states of the solute. For example, if ionic and covalent states are used to describe the solute, preferential stabilization of the ionic state by the solvent will give the adiabatic ground state more ionic character. In addition, the EVB method lends itself to proper

configurational sampling and converging free energy calculations, which makes it possible to evaluate nonequilibrium solvation effects,¹ as we discuss in section 8.

4. The Rate Constant

With the ability to evaluate potential surfaces and activation free energies for enzymatic reactions, we are ready to evaluate rate constants and explore dynamical effects. The basic quantity of interest is the rate constant for the rate-determining step, which we take to be k_{cat} of eq 1. Our starting point is the well-known expression

$$k = \kappa k_{\text{TST}} \quad (11)$$

in which k_{TST} is the rate constant from transition-state theory (TST),

$$k_{\text{TST}} = \frac{1}{2} \langle |\dot{x}| \rangle_{\text{TS}} \exp[-\Delta g^\ddagger \beta] / \int_{-\infty}^{x^\ddagger} \exp[-\Delta g(x)\beta] dx \quad (12)$$

and κ is the “transmission coefficient”. In eq 12, x again represents a generalized reaction coordinate, which we now consider to be a function of time; \dot{x} is the time-dependent velocity along x , x^\ddagger is the (time-independent) value of x at the TS, $\langle \dots \rangle_{\text{TS}}$ denotes a time average over periods in the region of the TS, and Δg^\ddagger is the activation free energy, $\Delta g(x^\ddagger)$.

In TST, the average velocity in the TS, $\langle |\dot{x}| \rangle_{\text{TS}}$, is equated to the mean velocity for one-dimensional translation in a thermally equilibrated system,

$$\langle |\dot{x}| \rangle_{\text{TS}} = (2\beta^{-1}/(\pi m))^{1/2} \quad (13)$$

where m is the reduced mass for this motion. With the additional assumptions that Δg is a harmonic function of x and that translation along x is in equipartition of energy with other motions of the system, k_{TST} can be simplified further to

$$k_{\text{TST}} \approx (\beta h)^{-1} \exp(-\beta \Delta g^\ddagger) \quad (14)$$

The time-dependent reaction coordinate $x(t)$ in eq 12 can be defined, in the same manner as the generalized reaction coordinate in eq 6, as the fluctuating energy gap between the reactant and product EVB states, $\Delta \epsilon(t) = \epsilon_2(t) - \epsilon_1(t)$. The time-dependent coordinate also can be divided into solute and solvent coordinates, $R(t)$ and $S(t)$, and the solvent component again can be related to the difference in electrostatic energies between the product and reactant states:⁴⁰

$$S(t) \propto \Delta \epsilon_{\text{el}}(t) = \epsilon_{\text{el},2}(t) - \epsilon_{\text{el},1}(t) \quad (15)$$

5. The Transmission Coefficient

The transmission coefficient (κ) in eq 11 is potentially the main source of dynamical effects. Much of the discussion of whether dynamical effects contribute to enzyme catalysis therefore has revolved around whether κ is higher in enzymes than in solution. If we neglect tunneling and other quantum effects for the moment, κ depends on two interrelated factors: the probability that a system arriving at x^\ddagger from the reactant side of the barrier will end up on the product side rather than regenerating the reactants, and the average number of times that a productive trajectory passes back and forth across x^\ddagger before it moves permanently to the product

side. These factors can be evaluated by examining a family of MD trajectories that start in the TS with a thermal distribution of velocities.^{7,45–52} The trajectories are propagated both forward and backward in time until both segments have settled in either the reactant or the product state, and the forward and backward segments are combined to obtain a complete trajectory. In an approach introduced by Keck,⁴⁵ κ is written

$$\kappa = \frac{\langle\langle H(\dot{x})\dot{x} \rangle_{\text{TS}}^{\xi}\rangle_{\pm}}{\langle\langle H(\dot{x})\dot{x} \rangle_{\text{TS}}\rangle_{\pm}} \approx \frac{\langle\langle H(\dot{x})\dot{x} \rangle_{\text{TS}}^{\xi}\rangle_{\pm}}{\left\langle \frac{1}{2}|\dot{x}| \right\rangle_{\text{TS}}} \quad (16)$$

Here $\langle\langle \dots \rangle_{\pm}$ denotes an average over many trajectories that start on either the reactant or product side of the barrier, reach the TS and possibly fluctuate in this region for a time, and are terminated when they leave the TS region. $H(\dot{x}(t))$ is a Heaviside step function that is unity for positive \dot{x} and zero for negative \dot{x} . The function ξ is defined as follows: if a trajectory crosses x^{\ddagger} n times with positive \dot{x} and $(n-1)$ times with negative \dot{x} , then $\xi = 1/n$; for all other trajectories, $\xi = 0$. This function counts only trajectories that begin on the reactant side and end in products, and it weights each of these inversely by the number of times the trajectory crosses x^{\ddagger} in the forward direction.

Another way of calculating the transmission coefficient, called the “reactive flux” method,^{47,50,53,54} is to evaluate the time-dependent function

$$\kappa(t) = \frac{\langle\langle \dot{x}(0)H(x(t) - x^{\ddagger}) \rangle_{\text{TS}}\rangle_{+}}{\langle\langle \dot{x}(0)H(\dot{x}(0)) \rangle_{\text{TS}}\rangle_{+}} \quad (17)$$

Here $\langle\langle \dots \rangle_{+}$ denotes an average over trajectories that begin at x^{\ddagger} and are propagated forward in time; the function $H(\dot{x}(0))$ is unity if the initial velocity along x is in the forward direction, and zero if the initial velocity is backward; $H(x(t) - x^{\ddagger})$ is unity if the trajectory is on the product side of x^{\ddagger} at time t ($x \geq x^{\ddagger}$) and zero if the trajectory is on the reactant side. $\kappa(t)$ is 1 at $t = 0$ and, in the simulations that have been described, decreases within 10–20 fs to a plateau that is taken to be the time-independent transmission coefficient.

The transmission factor also can be obtained by considering the average effective velocity with which productive trajectories cross the TS:^{30,40}

$$\langle\dot{x}_{\text{eff}}\rangle_{\text{TS}} = \Delta x^{\ddagger}/\tau_{+} \quad (18)$$

where Δx^{\ddagger} is an arbitrarily defined length of the TS on x and τ_{+} is the average time that productive trajectories take to traverse this region. If the system recrosses the barrier several times before it settles into P, $\langle\dot{x}_{\text{eff}}\rangle_{\text{TS}}$ will be smaller than the velocity given by eq 13, and κ will be less than unity. The transmission coefficient thus can be approximated as the ratio of $\langle\dot{x}_{\text{eff}}\rangle_{\text{TS}}$ to $\langle|\dot{x}|\rangle_{\text{TS}}$:

$$\kappa \approx \langle\dot{x}_{\text{eff}}\rangle_{\text{TS}}/\langle|\dot{x}|\rangle_{\text{TS}} = \Delta x^{\ddagger}\tau_{+}^{-1}(2\beta^{-1}/(\pi m))^{-1/2} \quad (19)$$

If Δx^{\ddagger} is defined identically for an enzymatic reaction and the reference reaction in solution, any significant difference between the transmission factors for the two processes must reflect a difference in τ_{+} . Further, since the solute is the same in the enzyme and solution, the difference in τ_{+} must originate in the interactions of the reacting groups with their surroundings in the two transition states.

If the relaxation time for solvent motions is equal to or longer than that for the solute dipole, as it probably is in most cases, τ_{+} is given to a good approximation by⁴²

$$\tau_{+}^{-1} \approx \frac{\partial\langle\Delta\epsilon_{\text{el}}(t)\rangle_{\text{TS}}}{\partial t}/\Delta x_{\text{S}}^{\ddagger} \quad (20)$$

where $\Delta x_{\text{S}}^{\ddagger}$ is the length of the TS region on the solvent component of x , $\Delta\epsilon_{\text{el}}(t)$ is the time-dependent solvent reaction coordinate (eq 15), and $\langle\Delta\epsilon_{\text{el}}(t)\rangle_{\text{TS}}$ is evaluated with a mapping potential that keeps the system in the region of the TS.

The average time dependence of the solvent reaction coordinate in the TS ($\langle\Delta\epsilon_{\text{el}}(t)\rangle_{\text{TS}}$ in eq 20) can be related to the electric dipole of the solute ($\bar{\mu}$) by starting with the coupled equations for the time dependence of the solvent and solute coordinates and using the linear-response approximation:^{40,55}

$$\langle\Delta\epsilon_{\text{el}}(t)\rangle_{\text{TS}} \approx \frac{\langle\Delta\epsilon_{\text{el}}^{\text{max}}\rangle \int_0^t \{\langle\Delta\dot{\epsilon}_{\text{el}}(t)\Delta\epsilon_{\text{el}}(t+\tau)\rangle_{\text{TS}}\langle\Delta\bar{\mu}(\tau)\rangle_{\text{TS}}\} d\tau}{\langle\Delta\bar{\mu}_{\text{max}}\rangle \langle\Delta\dot{\epsilon}_{\text{el}}(t)\Delta\epsilon_{\text{el}}(t)\rangle_{\text{TS}}} \quad (21)$$

In this expression, $\langle\Delta\bar{\mu}_{\text{max}}\rangle$ is the difference between the solute dipoles in the product and transition states ($\langle\Delta\bar{\mu}\rangle_2 - \langle\Delta\bar{\mu}\rangle_{\text{TS}}$), and $\langle\Delta\epsilon_{\text{el}}^{\text{max}}\rangle$ is the average change in $\Delta\epsilon_{\text{el}}$ between these two states ($\langle\Delta\epsilon_{\text{el}}\rangle_2 - \langle\Delta\epsilon_{\text{el}}\rangle_{\text{TS}}$). The integrand in the numerator is the product of the average dipole at time τ ($\langle\Delta\bar{\mu}(\tau)\rangle_{\text{TS}}$) and the response function $\langle\Delta\dot{\epsilon}_{\text{el}}(t)\Delta\epsilon_{\text{el}}(t+\tau)\rangle$, which is simply the negative of the time derivative of the autocorrelation function of $\Delta\epsilon_{\text{el}}$ itself ($C_{\text{el}}(\tau)$):

$$C_{\text{el}}(\tau) = \langle u_{\text{el}}(t)u_{\text{el}}(t+\tau) \rangle \quad (22a)$$

$$\frac{\partial C_{\text{el}}(\tau)}{\partial t} = \frac{\partial}{\partial t} \langle u_{\text{el}}(t)u_{\text{el}}(t+\tau) \rangle = -\dot{u}_{\text{el}}(t)u_{\text{el}}(t+\tau) \quad (22b)$$

where $u_{\text{el}}(t) = \Delta\epsilon_{\text{el}}(t) - \langle\Delta\epsilon_{\text{el}}\rangle$. The autocorrelation function is widely used in studies of solvation dynamics^{56–60} and, as discussed below, can be used to analyze the vibrational modes that are coupled to a reaction.

Despite the elegance of the reactive flux method (eq 17), we prefer to use the autocorrelation of the energy gap (eqs 18–22) because it provides a more direct connection to the view of the enzyme as an effective solvent for the reacting groups. Comparisons of calculated transmission coefficients for enzymatic and nonenzymatic reactions will be discussed in the following section.

6. The Autocorrelation Function of the Energy Gap Is Similar in Enzymes and Solution

To illustrate the use of the EVB approach to describe an enzymatic reaction in terms of the fluctuating energy gap, consider the $S_{\text{N}}2$ reaction catalyzed by haloalkane dehalogenase. This reaction involves a nucleophilic attack of a carboxylate group on the carbon of chloroethane.⁶¹ As shown schematically in Figure 2, the fluctuating dipoles of the solvent or protein can either stabilize or destabilize the product state relative to the reactant state and thus can modulate the chance that the solute will move to the product state.²⁸ The same point has been illustrated for many other systems.¹

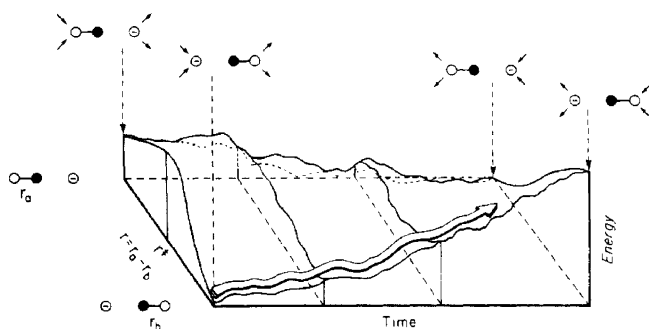


Figure 2. A schematic description of the role of the solvent fluctuations in a S_N2 reaction in which a nucleophile (\ominus) displaces a leaving group (\oplus) from a carbon atom (\bullet). The spatial coordinate (r) is the difference between the lengths of the bonds from the carbon to the attacking and leaving atoms (r_a and r_b). Solvent dipoles (\rightarrow) must reorient as the solutes move along the reaction path. Reprinted with permission from Hwang, J.K.; King, G.; Creighton, S.; Warshel, A. *J. Am. Chem. Soc.* **1988**, *110*, 5297–5311. Copyright 1988 American Chemical Society.

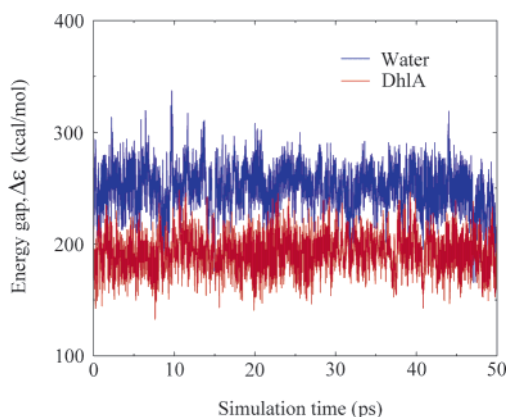


Figure 3. The energy gap between the diabatic product and reactant states in the reaction catalyzed by haloalkane dehalogenase (Dh1A) during MD simulations of the enzyme (red curves) and of the same reaction in water (blue curves). Reprinted with permission from Olsson, M. H. M.; Warshel, A. *J. Am. Chem. Soc.* **2004**, *126*, 15167–15179. Copyright 2004 American Chemical Society.

Nam et al.²³ recently examined haloalkane dehalogenase by a QM/MM molecular orbital approach. They focused on the force autocorrelation function, $C_F(t)$, which is a valid but somewhat less direct measure of the solvation dynamics than the autocorrelation function of the energy gap ($C(t)$). Nam et al. found that $C_F(t)$ relaxed more rapidly in the enzyme than in water and that the $C_F(t)$ of the enzyme had some oscillatory components that were not seen in water. The finding that $C(t)$ can be somewhat different in the enzyme and in water also was described in an earlier study of alcohol dehydrogenase by Villa and Warshel,¹ although the solvation dynamics were found to be similar. Nam et al.²³ did not provide a separate analysis for the solute and solvent coordinates, which is difficult to do in standard QM/MM studies. The solute contribution cannot be obtained reliably by simply omitting the solvent's electrostatic contribution to the QM/MM Hamiltonian, since this gives the gas-phase results, which generally are very different from the behavior of the solute in solution (see the discussion of a similar problem by Hwang et al.⁴⁰).

Figure 3 shows the calculated fluctuations of the energy gap between the reactant and product states during MD simulations of haloalkane dehalogenase and the reference system in water.⁶¹ The fluctuations of the solvent coordinates

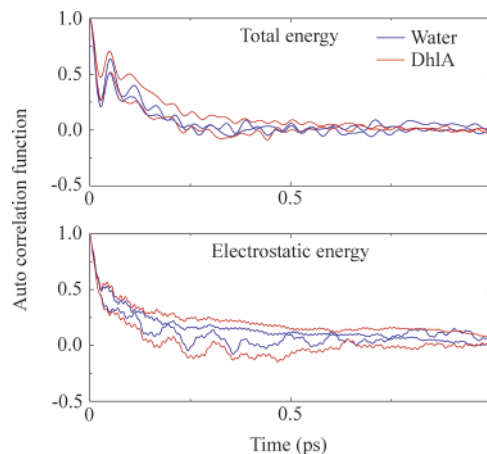


Figure 4. Autocorrelation function of the energy gap between the reactant and product states in the region of the TS in haloalkane dehalogenase (Dh1A, red curves) and the reference reaction in water (blue curves). Separate plots of the total energy and the electrostatic contribution to the energy are shown. The autocorrelation functions are normalized to 1 at zero time. Reprinted with permission from Olsson, M. H. M.; Warshel, A. *J. Am. Chem. Soc.* **2004**, *126*, 15167–15179. Copyright 2004 American Chemical Society.

in the enzyme and solution are quite similar. For a more definitive analysis, one can use the autocorrelation function of the energy gap with eqs 12–16 to compare the transmission coefficients of the enzyme and solution reactions. Figure 4 shows autocorrelation functions of the energy gap in the region of the TS for haloalkane dehalogenase and the reference reaction. The figure presents the autocorrelation functions of both the total gap, $C(t)$, and the electrostatic component that we take as the solvent coordinate, $C_{el}(t)$. It includes the results from two MD simulations of each system to show the variability of the results. Although the results depend somewhat on the initial positions and velocities in the trajectories, the decay kinetics of the autocorrelation function are very similar in the enzyme and water, indicating that the transmission coefficients are not significantly different in the two systems. In both cases, the system relaxes in about 0.1 ps. Similar results are obtained by direct simulations of the actual relaxation from the TS to the product state.^{40,62} These simulations give no indication that the enzymatic catalysis depends on dynamical effects.

7. The Relaxation Dynamics of the Effective Solute and Solvent Coordinates Are Similar in Enzymes and Solution

From the discussion above, it is clear that an analysis of the role of the enzyme as a solvent is important for understanding of enzyme catalysis. Descriptions of reacting systems in terms of effective solute and solvent coordinates have been used in early classifications of solvent effects⁶³ and in studies by Hwang et al.⁴⁰ that form the basis for the present discussion. The energy surfaces of the two EVB states can be described in terms of effective coordinates of the solute and solvent molecules as follows:

$$\begin{aligned} \epsilon_1 &\approx \sum_i \frac{\hbar\omega_i^r}{2} (r_i + \delta_i^r/2)^2 + \sum_j \frac{\hbar\omega_j^s}{2} (s_j + \delta_j^s/2)^2 \\ &\approx \frac{\hbar\omega_R}{2} (R + \delta_R/2)^2 + \frac{\hbar\omega_S}{2} (S + \delta_S/2)^2 + V_{\perp}(R_{\perp}, S_{\perp}) \end{aligned} \quad (23a)$$

$$\begin{aligned} \epsilon_2 &\approx \sum_i \frac{\hbar\omega_i^r}{2}(r_i - \delta_i^r/2)^2 + \sum_j \frac{\hbar\omega_j^s}{2}(s_j - \delta_j^s/2)^2 + \Delta V_0 \\ &\approx \frac{\hbar\omega_R}{2}(R - \delta_R/2)^2 + \frac{\hbar\omega_S}{2}(S - \delta_S/2)^2 + \Delta V_0 + \\ &\quad V_{\perp}(R_{\perp}, S_{\perp}) \quad (23b) \end{aligned}$$

$$\Delta\epsilon_{12} = \epsilon_2 - \epsilon_1 \approx \frac{-\hbar}{2}(\omega_S\delta_S S + \omega_R\delta_R R) + \Delta V_0 \quad (23c)$$

Here r_i and s_j represent normal mode coordinates of the solute and solvent, respectively; R and S are dimensionless effective coordinates for the solute and solvent; ω_i^r , ω_j^s , ω_R , and ω_S are the corresponding vibrational frequencies, δ_i^r , δ_j^s , δ_R , and δ_S are the displacements of the potential minima in ϵ_2 relative to ϵ_1 , and ΔV_0 is the difference between the minima of ϵ_2 and ϵ_1 . The dimensionless displacements are given by $\delta = (m\omega/\hbar)^{1/2}\Delta r$, where m is the reduced mass of the atoms that participate in the motion. $V_{\perp}(R_{\perp}, S_{\perp})$ represents contributions from modes that are orthogonal to the reaction coordinate and do not contribute to $\Delta\epsilon_{12}$.

The effective frequencies ω_S and ω_R in eqs 23a and 23b can be defined as

$$\omega = \int_0^{\infty} \omega P(\omega) d\omega \quad (24)$$

in which $P(\omega)$ is the normalized spectral density of the corresponding contribution to $\epsilon_2 - \epsilon_1$. The effective solute coordinate (R) represents the contribution of intramolecular bond stretching or bending to the energy gap. In the case of the Dh1A reaction, this is related to the ordinary reaction coordinate ($R' = R_2 - R_1$, where R_1 and R_2 are the lengths of the bonds that are compressed and extended in the reaction) by $R = R'(\omega_R m_R/\hbar)^{1/2}$, where m_R is the reduced mass for the normal mode that is the compression of R_1 and extension of R_2 . As discussed in section 3, the effective solute coordinate S can be defined in terms of the electrostatic contribution to the energy gap between the reactant and product states, $(\epsilon_2 - \epsilon_1)_{el}$:

$$-S = (\epsilon_2 - \epsilon_1)_{el}/(\hbar\omega_S\delta_S) \quad (25)$$

We leave further discussion of the normal modes to section 9 and focus here on the two effective coordinates, R and S . The displacements along these coordinates are related to the reorganization energy of the reaction, λ , by

$$\begin{aligned} \lambda = \lambda_R + \lambda_S &= \sum_i \frac{\hbar\omega_i^r}{2}(\delta_i^r)^2 + \sum_j \frac{\hbar\omega_j^s}{2}(\delta_j^s)^2 \approx \\ &\quad \frac{\hbar\omega_R}{2}(\delta_R)^2 + \frac{\hbar\omega_S}{2}(\delta_S)^2 \quad (26) \end{aligned}$$

An essentially equivalent, but perhaps more familiar definition of the solvent coordinate can be obtained in terms of the macroscopic reaction field ($\vec{\xi}_{rf}$) at the solute cavity:

$$-\hbar\omega_S\delta_S S = (\epsilon_2 - \epsilon_1)_{el} = (\vec{\mu}_1 - \vec{\mu}_2) \cdot \vec{\xi}_{rf} \quad (27)$$

where $\vec{\mu}_1$ and $\vec{\mu}_2$ are the dipole moments of the solute in the corresponding diabatic states.

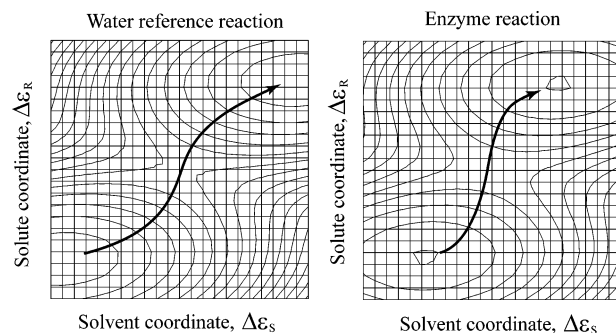


Figure 5. Contour plots of the total energy as functions of the solvent and solute reaction coordinates in the haloalkane dehalogenase reaction (right) and the reference reaction in water (left). Reprinted with permission from Olsson, M. H. M.; Warshel, A. *J. Am. Chem. Soc.* **2004**, *126*, 15167–15179. Copyright 2004 American Chemical Society.

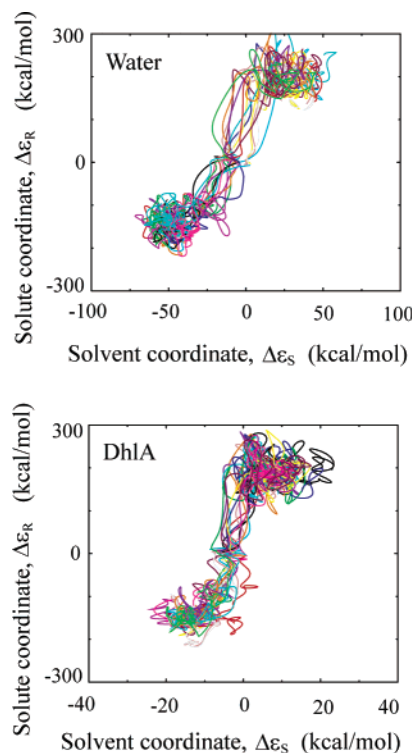


Figure 6. Downhill trajectories on the solvent and solute reaction coordinates starting from the transition state in the haloalkane dehalogenase reaction (lower) and the reference reaction in water (upper). Reprinted with permission from Olsson, M. H. M.; Warshel, A. *J. Am. Chem. Soc.* **2004**, *126*, 15167–15179. Copyright 2004 American Chemical Society.

Figure 5 shows calculated solute–solvent surfaces for haloalkane dehalogenase and the reference reaction in water.⁶¹ The distribution of the reorganization between the effective solute and solvent coordinates is somewhat different in the two systems, the solvent making a larger contribution in solution than in the enzyme. The overall picture, however, is similar in the two systems.

The most direct way to look for dynamical effects is simply to monitor the dynamics of the productive trajectories on the solute–solvent coordinate system. This can be done by propagating trajectories from the TS forward and backward in time as described in section 5. Figure 6 shows the behavior of a set of such trajectories for the haloalkane dehalogenase reaction.⁶¹ The dynamics in both the enzyme and solution are incoherent, the trajectories moving randomly

in the reactant state and occasionally acquiring enough thermal energy to move to the TS. As in Figure 5, the overall displacement on the solvent coordinate is larger in water than in the enzyme. However, the pertinent motions in both cases clearly occur in the solute–solvent space rather than simply the solute space. Further, the dynamics of relaxation from the TS to the product state are essentially the same in the enzyme and solution. Similar results have been obtained for alcohol dehydrogenase¹ and for the nucleophilic attack step in subtilisin.⁶⁴

In discussing haloalkane dehalogenase, Nam et al.²³ state, “In aqueous solution there is a significant electrostatic effect, which is reflected by the slow relaxation of the solvent. On the other hand, there is no strong electrostatic coupling in the enzyme and the major effect on the reaction coordinate motion is intramolecular energy relaxation.” This statement suggests that enzyme catalysis originates in part from an acceleration of the relaxation dynamics in the enzyme. Contrary to this notion, Figures 4–6 show that the relaxation dynamics on the solvent coordinate are similar in the enzyme and in water. Water is known to have a relatively short dielectric relaxation time constant compared to other solvents,⁵⁹ and relaxations of the solvent coordinate generally are, if anything, somewhat faster in water than in enzymes. Using eqs 11 and 18–22, one finds that the difference between the characteristic downhill times (τ_+) in the enzyme and solution has very little effect on the rate constant relative to the large effect of the different activation barriers.

Cui and Karplus⁶⁵ have examined the effect of the environment on motions in the TS for a proton-transfer reaction catalyzed by triosephosphate isomerase. They found that electrostatic effects of the environment reduce the curvature of the free energy surface both in the enzyme and in solution. The decreased curvature slows motion along the reaction coordinate. Although the effect on the downhill dynamics and transmission factor is small, the motions in the enzyme are slowed slightly more in the enzyme relative to solution. This is at odds with the suggestion by Nam et al.²³ that the motions are faster in the enzyme.

Cui and Karplus⁶⁶ also considered the possibility that dynamical effects could arise when vibrational equilibration is slow relative to the rate of crossing the barrier. This proposal will be discussed in section 9.

8. Nonequilibrium Solvation Does Not Contribute a Dynamical Effect

Some studies of reactions in solution have suggested that “nonequilibrium solvation” (NES) can affect the transmission factor for a reaction.^{1,7,67–71} In fact, Garcia-Viloca et al.⁷¹ recently suggested that these effects comprise a potentially important correction to transition-state theory and provide a key modern consideration for understanding enzymatic reactions (the nonequilibrium term of ref 71 includes the NES effect according to ref 190). However, NES is not really a dynamical effect or part of the transmission factor but rather a well-defined free energy factor (a part of Δg^\ddagger) that has been recognized for some time^{1,70,72} and has been included in almost all EVB studies since the introduction of eq 10. When the solute is at its TS, the solvent reorganization energy creates a barrier between the equilibrium configurations of the solvent in the reactant and product states. This barrier constitutes the entire activation free energy in outer-sphere electron-transfer reactions, and its contribution to Δg^\ddagger can be significant in other types of reactions as well.⁷⁰

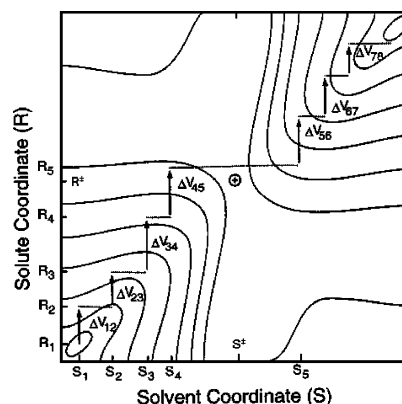


Figure 7. Contour plot of the potential surface for a reaction as a function of the solute (R) and solvent (S) coordinates. The closed oval contours at the lower left and upper right represent the reactant and product states; the $+$ at (R^\ddagger, S^\ddagger) indicates the TS. The arrows and dotted lines illustrate an attempt to calculate Δg^\ddagger by a free-energy perturbation approach using R as the mapping parameter. The mean change in potential energy resulting from changing the solute coordinate from R_i to R_j (ΔV_{ij}) is calculated during a trajectory on the mapping potential for R_i , while S is held at its equilibrium value for this mapping potential (S_i). At the end of this step, S is moved to its equilibrium value for the next trajectory (S_j) as indicated by the horizontal dashed line. This mapping procedure does not reflect the free-energy change for moving the solvent coordinate from S_i to S_j and does not sample the TS for the solvent coordinate (S^\ddagger), leading to an underestimate of the activation free energy (Δg^\ddagger). Reprinted from Warshel, A.; Parson, W.W. *Q. Rev. Biophys.* **2001**, *34*, 563–679 with permission from Cambridge University Press.

The contribution of NES to Δg^\ddagger is overlooked in treatments of reaction kinetics in which the solvent and solute coordinates are handled separately and the solvent is allowed to relax on its reaction coordinate during each step along the solute coordinate. Figure 7 illustrates such a treatment, in which the solute coordinate (R) is used as a mapping parameter. To move the system from the reactant state to the product state, a series of MD trajectories are run on the potential surfaces for intermediate values of R (R_1, R_2, \dots), while the solvent coordinate is allowed to fluctuate about its equilibrium value (S_i) for each R_i . The change in the potential of mean force (PMF) associated with changing R from R_i to R_j is calculated during a trajectory on R_i using the expression

$$\Delta g_{\text{PMF}}(R_j) - \Delta g_{\text{PMF}}(R_i) = -\beta^{-1} \langle \exp\{-\beta[E_g(R_j, S) - E_g(R_i, S)]\} \rangle_{E_g(R_i, S)} \quad (28)$$

When the reactant coordinate is changed to R_j , the equilibrium value of S changes from S_i to S_j , as indicated in Figure 7 by the horizontal dashed lines. The solvent therefore is still at S_4 at the end of the fourth mapping step but is at S_5 at the beginning of the fifth mapping step. The mapping procedure does not reflect the reorganization energy required to change the solvent coordinate between the mapping steps, and the transition state for the solvent coordinate (S^\ddagger) is never actually sampled. The resulting underestimate of Δg^\ddagger will be most serious if the coupling of the solute and solvent charges also is neglected. (As discussed above, when the solute charges are coupled to the field from the solvent charges and vice versa, the solute charges will differ from their gas-phase values at a given value of R .⁴⁰)

The contribution of NES to Δg^\ddagger can be studied by constraining the EVB solute to its TS geometry (R^\ddagger) and

using an FEP procedure to evaluate the free energy surface for moving along the solvent coordinate from its equilibrium configuration on one side of the TS to its equilibrium configuration on the other side (e.g., from S_4 to S_5 in Figure 7). The activation barrier attributable to NES is

$$\Delta g_{\text{NES}}^{\ddagger} = \Delta g_{\text{NES}}(R^{\ddagger}, S^{\ddagger}) - \Delta g_{\text{NES}}^0 \quad (29)$$

where

$$\Delta g_{\text{NES}}(R^{\ddagger}, S') = -\beta^{-1} \ln \langle \delta(S' - S) \exp\{-\beta[E_g(R^{\ddagger}, S) - E_0]\} \rangle_g \quad (30)$$

and Δg_{NES}^0 is the minimum value of Δg_{NES} . E_g denotes the ground-state energy surface obtained by diagonalizing the EVB Hamiltonian (eq 5), and E_0 is an arbitrary constant that cancels out in eq 29. The total activation free energy then can be approximated as

$$\Delta g^{\ddagger} \approx \Delta g_{\text{PMF}}^{\ddagger} + \Delta g_{\text{NES}}^{\ddagger} \quad (31)$$

where $\Delta g_{\text{PMF}}^{\ddagger}$ is the activation energy obtained by allowing the solvent to equilibrate at each value of R as illustrated in Figure 7.

Figure 8 shows calculations of the nonequilibrium solvation effect for a step in the reaction catalyzed by subtilisin, along with similar calculations for the corresponding process in solution.¹ Nonequilibrium solvation contributes about 4 kcal/mol to the barrier in solution and about 1 kcal/mol in the enzyme. The decrease in $\Delta g_{\text{NES}}^{\ddagger}$ can be viewed as one feature of the preorganized environment in the enzyme's active site. When eq 16 was used, direct simulations of downhill trajectories gave a transmission factor of approximately 0.6 for both the enzyme and the solution reaction, showing clearly that the NES effect is not a dynamical effect.

The EVB/FEP-US method described in section 3 incorporates the NES effect automatically by calculating the probability of finding the system at the transition state of the solute-solvent system, without having to divide Δg^{\ddagger} explicitly into equilibrium and nonequilibrium components.⁴⁰ The EVB Δg^{\ddagger} therefore should differ from $\Delta g_{\text{PMF}}^{\ddagger}$ by approximately $\Delta g_{\text{NES}}^{\ddagger}$.^{64,73}

Neria and Karplus⁷ have discussed effects of NES on the proton-transfer step in triosephosphate isomerase. They used EVB simulations of a "frozen-solvent" model described by Hynes and co-workers,^{68,74} in which fluctuations of the solvent are assumed to be much slower than those of the solute. In this model, the rate constant is written

$$k \approx \kappa_{\text{froz}} k_{\text{PMF}} \quad (32)$$

$$k_{\text{PMF}} = (\beta h)^{-1} \exp(-\beta \Delta g_{\text{PMF}}^{\ddagger}) \quad (33)$$

$$\kappa_{\text{froz}} = \langle \exp\{-\beta \Delta V\} \rangle_S \quad (34)$$

$$\Delta V = E_g(R_i^{\text{peak}}, S_i) - E_g(R^{\ddagger}, S^{\ddagger}) \quad (35)$$

Here $\Delta g_{\text{PMF}}^{\ddagger}$ is the activation potential of mean force given by eq 28, and $R_i^{\text{peak}}(S_i)$ is the value of the solute coordinate (R) at which the ground-state energy surface (E_g) goes through a maximum for a given fixed value of the solvent coordinate, S_i , (see Figure 9).^{68,74} Neria and Karplus⁷⁵ and

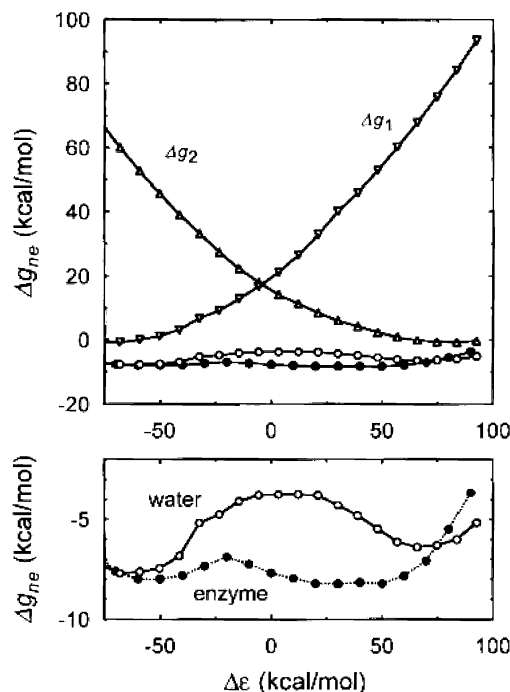


Figure 8. Nonequilibrium solvation barriers for the nucleophilic-attack step in subtilisin and the corresponding reaction in water. The free energy was calculated by keeping the solute in its TS geometry (R^{\ddagger} in Figure 7) and using a free-energy perturbation procedure to evaluate Δg for moving the solvent across the TS as illustrated by the path from S_4 to S_5 in Figure 7. The mapping procedure allowed the solute charges to evolve from their equilibrium values at (R^{\ddagger}, S_4) to the values at (R^{\ddagger}, S_5). The curves labeled Δg_1 and Δg_2 in the upper panel are the calculated contributions of nonequilibrium solvation to the free energy of the diabatic reactant and product states in water. The open and filled circles are the calculated contributions of nonequilibrium solvation to the adiabatic ground-state surfaces in water and the enzyme, respectively. The lower panel shows the adiabatic free energies on an expanded scale. Reprinted with permission from Warshel, A.; Bentzien, A. *ACS Symp. Ser.* **1999**, 721, 489–498; Villà, J.; Warshel, A. *J. Phys. Chem. B* **2001**, 105, 7887–7907; and Warshel, A.; Parson, W. W. *Q. Rev. Biophys.* **2001**, 34, 563–679. Copyright 1999 American Chemical Society.

Gertner et al.^{68,74} earlier had used κ_{froz} as the transmission coefficient for charge-transfer reactions in water and had concluded that it was determined by the rate of relaxations of the water around the reacting species.

Neria and Karplus⁷ compared the forces along the reaction coordinate when they constrained the motions of either the reacting solute or the protein in the frozen-solvent model. In contrast to the conclusions of Gertner et al.⁷⁴ for charge-transfer reactions in solution, they concluded that the dynamics of leaving the TS region in triosephosphate isomerase are not limited by relaxations of the protein but rather depend on rapid intramolecular motions of the solute within a relatively rigid cage.

The possible difference in the role of solvent relaxations in triosephosphate isomerase compared to charge-transfer reactions in solution was taken as an indication of the importance of dynamic effects in the enzyme. In our opinion such a conclusion would be unwarranted, since the analysis that Neria and Karplus used for the enzyme was not applied to the same reaction in solution. In addition, eq 32 is problematic because the rate constant actually is determined by Δg^{\ddagger} (including the contribution from $\Delta g_{\text{NES}}^{\ddagger}$), not $\Delta g_{\text{PMF}}^{\ddagger}$. $\Delta g_{\text{PMF}}^{\ddagger}$ differs from Δg^{\ddagger} in that it is evaluated without the

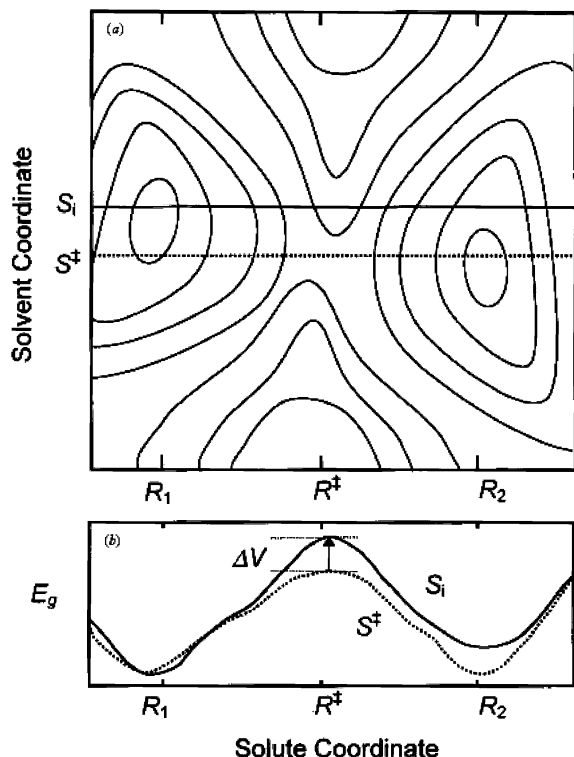


Figure 9. The frozen solvent model. Panel a is a contour plot similar to that of Figure 7 but for a system in which the solvent configurations are similar in the reactant and product states (note that here S is the ordinate). The horizontal solid or dotted lines represent reaction paths in which S is held fixed; S^{\ddagger} denotes the path with the smallest barrier. Panel b shows the potential energies along two such paths and indicates the meaning of ΔV in eq 35. Reprinted from Warshel, A.; Parson, W. W. *Q. Rev. Biophys.* **2001**, *34*, 563–679 with permission from Cambridge University Press.

$\delta(S-S')$ factor that appears in eqs 9, 10, and 30, which could lead to an underestimate of the energy barrier (see eq 28). The proper correction to the PMF rate constant is not κ_{froz} , but rather $\exp(-\beta\Delta g_{\text{NES}}^{\ddagger})$ (see eq 31). κ_{froz} may have no simple quantitative relation to either $\Delta g_{\text{NES}}^{\ddagger}$ or the usual transmission coefficient (κ), which must be evaluated in the full solute–solvent coordinate space unless the solvent is completely frozen. It is worth noting also that the simulations that underlie the frozen-solvent model^{67,76} neglect effects of the solvent on the charge distribution in the solute.⁴⁰ The underlying assumption that fluctuations of the protein environment are much slower than motions of the solute seems likely to be unrealistic, considering the results for Dh1A described above and for other systems.^{1,61}

Cannon et al.⁷⁷ have suggested that enzymes may catalyze reactions by removing a slow component of the reorganization on the solvent coordinate. Although decreasing the solvent reorganization energy can lower Δg^{\ddagger} and thus clearly can contribute to catalysis, there is no compelling evidence that this reflects a dynamical effect. Both experimental and theoretical studies have shown that the motions associated with reorganization of the first solvation sphere in water are extremely fast,^{57–59} and as shown in Figures 4 and 6, the same is true for the pertinent motions in proteins. Since the fast motions occur on the same time scales in proteins as in solution, removal of slow motions is unlikely to result in significant dynamical effects.

In conclusion, a critical analysis of nonequilibrium solvation effects shows that the nature of these effects are similar in enzymes and in solution. The main differences

appear to be associated with magnitude of the reorganization energy rather than with dynamical effects.

9. The Frequencies of Catalytically Important Vibrational Modes in Enzymes Are Similar to Those in Solution

The EVB approach allows one to evaluate the projections of protein or solvent motions along the reaction coordinate. In the “dispersed-polaron” or “spin-boson” treatment, this is done by relating the fluctuations of $\Delta\epsilon_{12}$ during an MD trajectory to the fluctuations of an equivalent harmonic system. We start with the autocorrelation function of the total energy gap,

$$C_i(\tau) = \langle u(t)u(t+\tau) \rangle \quad (36)$$

where $u(t) = \Delta\epsilon_{12}(t) - \langle \Delta\epsilon_{12} \rangle$. According to the Wiener–Khinchin theorem, the power spectrum of the fluctuations in a given diabatic state, $J(\omega)$, can be obtained from the Fourier transform of the autocorrelation function:

$$J(\omega) = \left| \int_{-\infty}^{\infty} C(t) \exp(i\omega t) dt \right| \quad (37)$$

$J(\omega)$ has peaks at the frequencies of the modes that are coupled to the reaction (ω_j), and in the high-temperature limit, the amplitudes of these peaks are proportional to the square of the displacement of the corresponding coordinate in ϵ_2 relative to ϵ_1 (The δ_i^r and δ_j^s in eqs 23a and 23b):⁵⁶

$$J(\omega) = \pi\beta^{-1} \sum_j \hbar\omega_j \delta_j^2 \delta(\omega - \omega_j) \quad (38)$$

where index j now runs over the normal modes of both the solute and the solvent, and $\delta(\omega - \omega_j)$ is the Kronecker delta function. The Fourier magnitudes obtained by eqs 37 and 38 can be scaled by relating the area under the spectral density function to the overall reorganization energy (λ) as in eq 26:

$$\lambda = \frac{1}{2} \sum_j \hbar\omega_j \delta_j^2 = \frac{\beta}{2\pi} \left| \int_{-\infty}^{\infty} J(\omega) d\omega \right| \quad (39)$$

The reorganization energy can be obtained independently from the difference between the average values of $\Delta\epsilon_{12}$ during MD trajectories in the reactant and product states:

$$\lambda = \frac{1}{2} |\langle \epsilon_{12} \rangle_1 - \langle \epsilon_{12} \rangle_2| \quad (40)$$

and also can be related to the variance of the distribution of $\Delta\epsilon_{12}$.

Figure 10 shows an analysis along these lines for the vibrations that are coupled to the haloalkane dehalogenase reaction. A similar analysis has been given for other reactions.^{1,78,79} In all the cases that we have examined, the power spectrum of the projection of the solvent vibrations on the reaction coordinate is similar in the enzyme and the reference reaction in water.

Normal-mode analysis is a useful approach for analyzing how the protein perturbs motions of the solute, although it may be less effective for dealing with highly anharmonic motions of the solvent. Go and co-workers⁸⁰ have used this approach for evaluating the Franck–Condon factors for electron-transfer reactions of cytochrome *c*. Cui and Karplus^{65,66} have used a normal-mode analysis to examine the

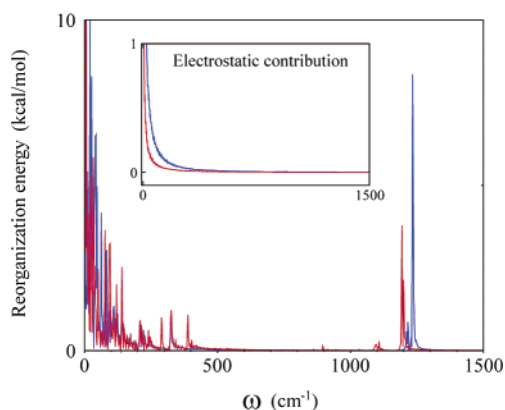


Figure 10. Fourier transform of the autocorrelation function of the energy gap between the product and reactant states in the haloalkane dehalogenase reaction (red) and a reference reaction in water (blue). Reprinted with permission from Olsson, M. H. M.; Warshel, A. *J. Am. Chem. Soc.* **2004**, *126*, 15167–15179. Copyright 2004 American Chemical Society.

projections of some of the modes of the protein–substrate system on the reaction coordinate in triosephosphate isomerase. They note that motions that raise the energies of the reactant and product symmetrically (“promoting modes”) favor the reaction, while modes that affect the energies asymmetrically (“demoting modes”) oppose it. These are basically thermodynamic effects that reflect the height and shape of the barrier for proton transfer. In general, rather than altering the dynamics of moving through or relaxing from the TS, a promoting or demoting mode simply reflects the shape of the potential surface along a particular coordinate.

Cui and Karplus⁶⁵ suggest that certain modes could affect the transmission coefficient and thus might have a dynamical effect, if vibrational equilibration is slow relative to the rate of crossing the barrier. They argue that this condition is met because crossing the barrier for the proton-transfer step in triosephosphate isomerase takes only about 30 fs, whereas the full redistribution of vibrational energy would take much longer. They nevertheless agree that any dynamical effect is likely to be minor since the transmission coefficient probably is at least 0.5.

The idea that increasing the rate of vibrational equilibration could lead to dynamical effects merits some additional discussion. We are not aware of any formal expression that relates consistently the quantum mechanical transmission factor to the classical time of crossing the TS or the rate of energy redistribution. In a classical picture, the speed of a single crossing of the TS is constant; what counts is the time required to dissipate an amount of energy in the order of $k_B T$ and thus to make the barrier crossing effectively irreversible. As eqs 19–21 show, the relevant relaxation time for this process is determined by the relaxation of the solvent coordinate, rather than that of the solute. With a solvent reorganization energy of about 20 kcal/mol for triosephosphate isomerase⁸¹ and a typical relaxation time of ~ 100 fs for the autocorrelation function in enzymes (see Figure 4), a relaxation of $\Delta\epsilon_{12}$ by $k_B T$ requires only about 5 fs. The time required probably is somewhat longer than this, since the inertial relaxation time deduced from $C(t)$ does not reflect a complete vibrational equilibration.⁶² Nevertheless, we have here a picture of fast solvent relaxation in both the enzyme and solution, which means that changes in the rate of this relaxation are unlikely to contribute significantly to catalysis.

In a semiclassical model, one can treat the solute vibrations quantum mechanically and consider semiclassical surface

crossing between the solute states under the perturbation of the classically fluctuating environment.^{31,82} Although such a treatment is fully valid only in the diabatic limit, it is a useful way to view environmental effects in proton-transfer processes.^{82–85} As discussed earlier in this section, the protein or water surrounding the reacting species usually provides a quasicontinuum of modes with a wide range of frequencies and coupling strengths. Energy redistribution comes into play only through the autocorrelation of the energy gap, which typically decays most of the way to zero in about 50 fs as modes with different frequencies get out of phase.⁸⁶

Coherent dynamical effects do occur in photobiological processes such as the primary electron-transfer step in photosynthetic bacterial reaction centers, where an ensemble of molecules can be excited coherently with a short pulse of light. In this system, electron transfer occurs from the excited state on the same time scale as relaxation among the solvent modes that are coupled to the reaction. Vibrational coherence can result in oscillatory kinetics and deviations from the predictions of Marcus theory.^{62,86–89} Related dynamical effects also have been seen in ground-state organic reactions that proceed from an instantaneously generated intermediate.⁹⁰ However, such effects are not likely to operate in thermally activated barrier-crossing events, where the equilibrium energy distribution usually appears to determine the rate constant.

10. Tunneling and Other Nuclear Quantum Mechanical Effects Do Not Contribute to Catalysis in a Major Way

Studies of isotope effects on some enzymatic reactions have pointed to nuclear tunneling and other nuclear quantum mechanical effects such as zero-point energy contributions of the participating vibrational modes.⁹¹ These findings frequently have been interpreted as evidence for dynamical effects. An enzyme might, for example, exploit a particular vibrational mode that modulates the thickness of the barrier through which an atom can tunnel.

One sign of nuclear tunneling is a reaction rate that becomes independent of temperature at low temperatures, when the available thermal energy is insufficient to populate the transition state. Several of the electron-transfer steps in photosynthetic reaction centers exhibit such kinetics at low temperature and have been interpreted as reflecting nuclear tunneling although they probably occur partly from hot vibrational levels that are populated by the excitation pulse.^{62,92} To our knowledge, however, temperature-independent kinetics has not been described for any ground-state enzymatic reactions.

Isotope effects also can provide indications of nuclear tunneling. In the absence of tunneling, a primary isotope effect commonly is ascribed to a change in the zero-point energy of a bond that is broken in the rate-limiting step of a reaction. The zero-point energy of a harmonic vibration of a system with reduced mass m and force constant f is $1/2\hbar\omega = 1/2\hbar(f/m)^{1/2}$. If the vibration involves a C–H, N–H, or O–H bond, the reduced mass will be approximately equal to the mass of the H atom ($m = 1$), so replacing protium by a heavier atom of mass m_2 (deuterium or tritium) will decrease the zero-point energy by a factor of approximately $m_2^{-1/2}$. The dependence of the vibrational energy on m vanishes at the TS, where the slope of the potential energy surface is zero. The isotopic substitution should, therefore,

increase the activation enthalpy by $\Delta\Delta H^\ddagger \approx 1/2\hbar f^{1/2}(1 - m_2^{-1/2})$. Neglecting any changes in the preexponential factor, the transition-rate theory thus predicts that the rate constants measured with protium, deuterium, and tritium (k_H , k_D , and k_T) will be related by the expression

$$\frac{\ln(k_H/k_T)}{\ln(k_D/k_T)} \approx \frac{1 - 3^{-1/2}}{2^{-1/2} - 3^{-1/2}} \approx 3.3 \quad (41)$$

(See Swain,⁹³ Saunders,⁹⁴ Antoniou and Schwartz,²⁴ Kohen and Klinman,⁹⁵ and Cui and Karplus⁶⁶ for additional discussion.)

Isotopic substitutions should have larger effects on the rate constants of reactions that involve nuclear tunneling, which in simple models depends exponentially, rather than linearly, on $m^{-1/2}$. Thus a primary isotope effect in which the ratio $\ln(k_H/k_T)/\ln(k_H/k_D)$ exceeds the value of 3.3 predicted by eq 41 is often taken as a sign of tunneling. (A “primary” isotope effect refers to isotopic substitution of an atom that participates directly in a bond that is broken in the reaction; “secondary” effects are those resulting from substitution of a neighboring atom). Klinman and co-workers have measured ratios exceeding 3.3 in alcohol dehydrogenases,^{18,96,97} serum amine oxidase,⁹⁸ lipoxygenase,⁹⁹ and glucose oxidase.¹⁰⁰ In one study, Kohen et al.¹⁸ found that the isotope effects on alcohol dehydrogenase from a thermophilic microorganism, *Bacillus stearothermophilus*, decreased in magnitude with increasing temperature, in accord with the expectation that contributions to the total rate from tunneling will decrease in importance as thermally excited excursions over the barrier become more frequent. However, the ratio $\ln(k_H/k_T)/\ln(k_D/k_T)$ for secondary isotope effects increased with temperature above 30 °C. The authors concluded that protein fluctuations are essential for tunneling in alcohol dehydrogenase and that in the enzyme from *B. stearothermophilus*, these fluctuations are most effective at the elevated temperatures at which the organism thrives. This would be in line with previous suggestions that the conformational flexibility of proteins from thermophilic organisms at high but physiologically appropriate temperatures is comparable to that of the homologous proteins from mesophilic organisms at their physiologically appropriate lower temperatures.^{13,101} The shifted temperature dependence of protein flexibility in thermophiles does not, however, necessarily imply that a particular amount of flexibility is needed for enzyme activity at the physiological temperature. It could just reflect the need to keep proteins from unfolding under physiological conditions. An organism that lives at high temperatures could achieve a given reaction rate even if Δg^\ddagger is higher than it is in a mesophile, since k_{cat} depends on $\exp(-\Delta g^\ddagger/(k_B T))$.

Kohen et al.¹⁸ made the interesting observation that the activation enthalpy (ΔH^\ddagger) for the reaction of the thermophilic alcohol dehydrogenase decreased from 23.6 kcal/mol at low temperatures (0–30 °C) to 14.6 kcal/mol at higher temperatures (30–65 °C). They interpreted this observation as supporting a contribution to k_{cat} from vibrationally enhanced tunneling at higher temperatures. The activation free energy, however, remained essentially constant. In TST, this means that a compensating increase in $-T\Delta S^\ddagger$ accompanies the decrease in ΔH^\ddagger as the temperature is raised (Figure 11a). Such enthalpy–entropy compensation is seen in many nonenzymatic systems, where it usually is ascribed to a balance between enthalpic and entropic components of solvation (see Hwang et al.,⁴⁰ Anderson,⁵⁴ and Levy and Gallicchio¹⁰² for recent reviews).

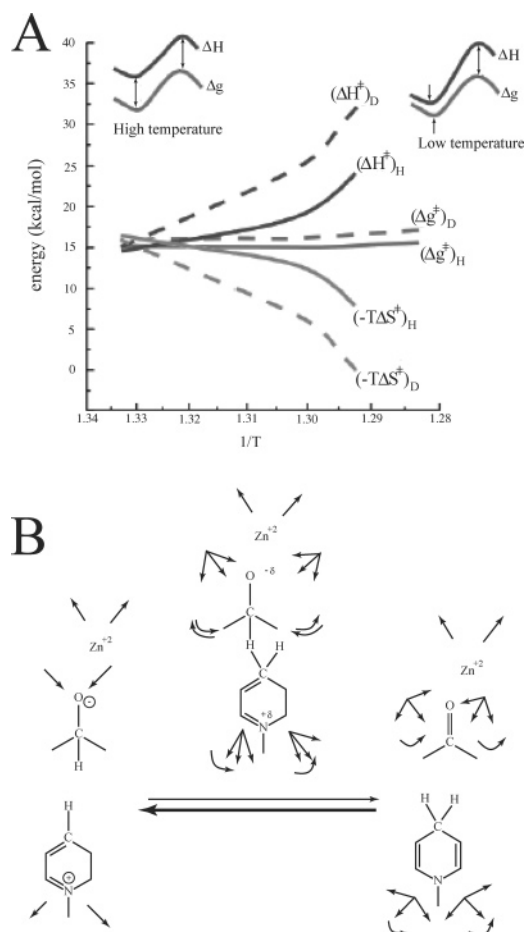


Figure 11. A schematic thermodynamic analysis of the reaction catalyzed by the alcohol dehydrogenase of *B. stearothermophilus* (A) and a rationalization of these data (B). Panel A illustrates the experimental fact that if changes in ΔH^\ddagger and $-T\Delta S^\ddagger$ with temperature compensate for each other, the activation free energy will be essentially independent of temperature. Panel B considers the reaction (from left to right) and suggests that the entropy changes could reflect restrictions on fluctuations of protein dipoles in the highly polar reactant state relative to the partially polar TS (thus leading to a positive ΔS^\ddagger). Raising the temperature is expected to make ΔS^\ddagger less positive since this would release some of the frozen motions in the reactant state.

The observed decrease in ΔS^\ddagger with temperature in the alcohol dehydrogenase reaction can be rationalized by considering the expected interactions of the solute with its surroundings. Because the reaction in the direction considered by Kohen et al.¹⁸ proceeds from a polar ion pair through a less polar TS to a nonpolar product (see Figure 11b), motions of the surroundings are expected to be less restricted in the TS than in the reactant state, contributing a positive term to ΔS^\ddagger . Raising the temperature will release some of the motions that are frozen in the reactant state, which should make ΔS^\ddagger less positive. This description is testable by computer simulations using a restraint–release approach of the type described by Villà et al.¹⁰³ In the absence of such simulations, we see no need to invoke dynamical effects to explain the temperature dependence of ΔH^\ddagger .

The enzyme lipoxygenase, which catalyzes addition of O_2 to an unsaturated fatty acid, exhibits unusually large kinetic isotope effects with k_H/k_D ratios that range from about 70 at 310 K to approximately 100 at 278 K.^{99,104–106} The rate-limiting step in the reaction is transfer of a hydrogen from the fatty acid to an iron cofactor on the enzyme.¹⁰⁷ Knapp et al.,⁹¹ Liang and Klinman,²⁷ and Hatcher et al.¹⁰⁸ have

emphasized the importance of obtaining a correct prediction of the temperature dependence for this enzyme, in which tunneling appears to play a major role. As far as we are aware, there are no published simulation studies that accurately reproduce the temperature dependence of $\ln(k_H/k_T)/\ln(k_D/k_T)$ over a wide range of temperatures for lipoxxygenase, the thermophilic alcohol dehydrogenase, or any other enzyme. As discussed by Olsson et al.,⁷⁹ it is much harder for microscopic simulations to capture the quantitative temperature dependence of kinetic isotope effects than it is to calculate activation free energies. The problem is related to the well-known difficulty of obtaining entropic effects by direct simulations. Because the isotope effect depends strongly on the average donor–acceptor distance, it is difficult to get its temperature dependence quantitatively unless one can get the exact temperature dependence of this distance. Doing this by MD simulations is particularly difficult when the free energy surface is relatively flat. The complicated temperature dependence of the isotope effects in the thermophilic alcohol dehydrogenase, for example, could reflect entropy–enthalpy compensation as discussed above. Changing the average donor–acceptor distance by 0.5 Å often costs very little free energy and gives only small errors comparable to the experimental uncertainty in the activation free energy (approximately ± 0.5 kcal/mol) but can result in a large error in the temperature dependence of the isotope effect. But the difficulty of obtaining converging results in such simulations means only that we presently cannot obtain a unique interpretation of the isotope effect, not that the effect reflects dynamical contributions to catalysis. Cui and co-workers^{65,66,109} found no consistent correlation between the ratio $\ln(k_H/k_T)/\ln(k_D/k_T)$ and calculated corrections to the rate constant from nuclear tunneling in horse liver alcohol dehydrogenase and triosephosphate isomerase.

Although calculating the temperature dependence of kinetic isotope effects remains a challenge, we feel that getting the correct activation free energies and rate constants for the enzyme and solution reactions is more critical from the perspective of enzyme catalysis. As we discuss in more detail below, current computational approaches appear to be sufficiently accurate for this task, even for lipoxxygenase and other enzymes where nuclear tunneling is important.

The problems associated with interpreting the temperature dependence of kinetic isotope effects are highlighted by a recent discussion⁹¹ of the I553A mutant of soybean lipoxxygenase. The temperature dependence of the kinetic isotope effect differs markedly between the wild-type and mutant enzymes. It was suggested that the I553A mutation weakens compression of the donor–acceptor distance by the enzyme and thus leads to “less optimized environmental dynamics.” However, the mutant and wild-type enzymes have essentially identical kinetic parameters (k_{cat} and K_m). The altered dynamics thus evidently have little effect on catalysis.

The idea that fluctuations of the protein are crucial for inducing nuclear tunneling is sometimes presented as a special feature of enzymes.^{24,25} For example, it has been suggested that evolutionary tuning of particular vibrational modes could explain why enzymes are more effective than catalytic antibodies.^{18,95} To analyze such proposals, it is necessary to have a microscopic approach for simulating nuclear quantum mechanical effects in proteins and solution. The simplest approach is to use a vibronic treatment similar to the dispersed-polaron treatment (eqs 9–10). A semiclas-

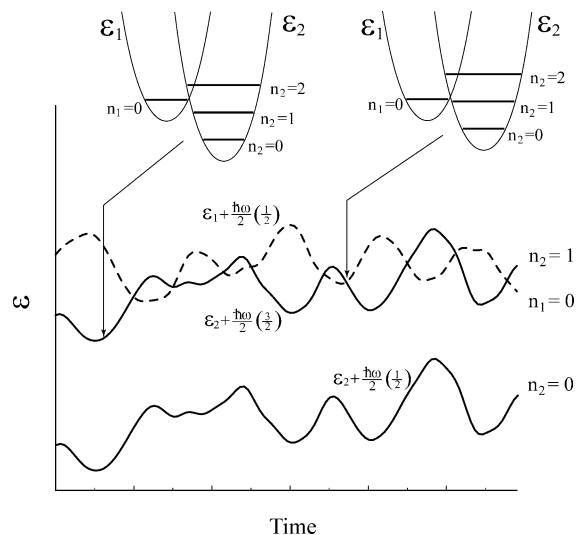


Figure 12. A semiclassical vibronic treatment of proton transfer. This model, which is valid only for small H_{12} , treats the carbon–proton stretching vibration quantum mechanically and the rest of the system classically. In this way, we monitor the energy gap between the vibronic states $\epsilon_1 + \hbar\omega_H/2(n_1 + 1/2)$ and $\epsilon_2 + \hbar\omega_H/2(n_2 + 1/2)$ for trajectories of the system with a fixed X–H bond length (see ref 83 for a related treatment). The figure depicts the time dependence of ϵ_1 and ϵ_2 plus zero or one excitation of the X–H bond and also provides the energy levels at two points on the trajectory. A semiclassical surface-hopping treatment of the crossing probability between the vibronic states, due to the fluctuating energy gap, leads to eq 43 (see ref 82).

sical EVB treatment along these lines, in which the stretching vibration of the carbon–proton bond is treated quantum mechanically while other modes are considered classically, is illustrated in Figure 12. The semiclassical microscopic rate constant obtained in this way ($k_{1m,2m'}$) represents the probability per unit time that a system in vibrational state m on the reactant side of the barrier will cross to vibrational state m' on the product side. This is given by

$$k_{1m,2m'} = \frac{H_{12}F_{mm'}}{\hbar} \left[\frac{\pi\hbar^2}{k_B T \lambda_{cl}} \right]^{1/2} \exp\left(-\frac{\Delta g_{mm}^\ddagger}{k_B T}\right) \quad (42)$$

where $F_{mm'}$ is the nuclear overlap integral for the transition and λ_{cl} is the classical reorganization energy of the solvent. Weighting $k_{1m,2m'}$ by the Boltzmann population of state m and summing over all the vibrational levels gives the overall rate constant:

$$k_{12} = \sum_{m,m'} k_{1m,2m'} \exp\left\{-\sum_i \frac{\hbar\omega_i}{k_B T} (m_i + 1/2)\right\} / \sum_m \exp\left\{-\sum_i \frac{\hbar\omega_i}{k_B T} (m_i + 1/2)\right\} \quad (43)$$

where ω_i is the frequency of vibrational mode i of the quantum system and m_i is the number of phonons of mode i in vibrational state m . In the high-temperature limit, the activation free energy (Δg_{mm}^\ddagger) for this model can be approximated by^{82,83}

$$\Delta g_{mm}^\ddagger \approx [\Delta G^\circ + \sum_i \hbar\omega_i (m'_i - m_i) + \lambda_{cl}]^2 / (4\lambda_{cl}) \quad (44)$$

A vibronic treatment of this type was developed originally by Kuznetsov and Ulstrup,¹¹⁰ and a somewhat more consistent formulation was introduced by Warshel and co-workers,⁸² who used a free energy term (ΔG°) rather than ΔE and clarified the relationship to the spectral distribution function. An extension to the low-temperature limit also was also obtained.⁸² Borgis and Hynes^{85,111} and Antoniou and Schwartz²⁴ have used similar treatments that consider only the lowest vibrational levels of a proton, and Knapp et al.^{91,105} have used this approach to study kinetic isotope effects in soybean lipoxygenase.

Equations 42–44 are strictly valid only in the diabatic limit when $|H_{12}F_{mm'}|$ is sufficiently small. In proton-transfer processes, H_{12} usually is far too large for this treatment to be reliable. However, if the displacement of the proton is substantial, $|F_{mm'}|$ can be quite small for 0–0 transitions since it is given by $F_{00} = \exp(-\delta^2/4)$, where δ is the dimensionless origin shift for the proton transfer ($\delta = (m_H\omega/\hbar)^{1/2}\Delta r$, where ω and m_H are the frequency and reduced mass for the X–H stretching mode). If the largest contribution to the rate constant comes from the 0–0 term, we, therefore, can use eq 42 as a rough estimate.

Determining the magnitude of the parameters in eq 42 raises two additional problems. First, if we consider a collinear proton transfer and treat all coordinates except the X–H stretching classically, we have to deal with the large intramolecular reorganization energy of this mode. Second, the effective frequency for the X–H stretch can be much smaller than the typical frequency of about 3000 cm^{-1} once the X \cdots Y distance becomes less than about 3.2 Å, when H_{12} can affect the ground-state curvature drastically. To correct for this, Warshel and Chu⁸² suggested modifying the diabatic potential to make it closer to the adiabatic potential. As long as the main contribution to the rate constant comes from the 0–0 term, it seems reasonable to use a linear approximation for the reduction in ω as the X \cdots Y distance is reduced. The overall rate constant reflects an integral over different X \cdots Y distances (different values of R in the present notation), and thus we can write

$$\bar{k}_{12} = \int k_{12}(R) \exp\{-\beta\epsilon(R)\} dR \quad (45)$$

where ϵ is the potential of mean force for the X \cdots Y distance.

In this model, the kinetic isotope effect depends on the increase in δ , and the resulting decrease in $|F_{00}|^2$ when H is replaced by deuterium or tritium. As discussed above, large kinetic isotope effects frequently are taken as evidence for quantum effects. But since the vibrational frequency (ω) that enters into δ decreases as the reacting groups are compressed, it appears that the isotope effect can be reduced, rather than increased, as the X \cdots Y distance is compressed. This is in clear contrast to the idea that compression by the enzyme increases tunneling.¹¹² In any event, one must keep in mind that the use of eq 43 could be entirely unjustified in many cases.

The use of phenomenologically fitted reorganization energies in eqs 42–45 merits some comment. In general, λ_{cl} in eq 44 represents the reorganization energy associated with all the modes that are not treated quantum mechanically. This should include both the outer-sphere reorganization energy ($\lambda_{\text{cl,out}}$) and the classical contributions to the inner-sphere reorganization energy ($\lambda_{\text{cl,in}}$). The outer-sphere reorganization energy, which is the most crucial parameter for a comparison of the enzyme and solution reactions, cannot be

estimated by simply fitting the predictions of eq 43 to experimental kinetic information, since the measured and calculated rates both include $\lambda_{\text{cl,in}}$ as well. Continuum models for estimating $\lambda_{\text{cl,out}}$ are problematic because the protein structure and its reorganization are not represented explicitly.¹¹³ Estimates of $\lambda_{\text{cl,in}}$ also can be unreliable because they are strongly model-dependent, as are the diabatic energies.

The reorganization energy of the lipoxygenase reaction has been estimated recently by two groups of investigators.^{91,108} Although both groups found a value of about 20 kcal/mol, this agreement appears to be fortuitous because Knapp et al.⁹¹ used eqs 42–45 and treated only the hydrogen stretching mode quantum mechanically, while Hatcher et al.¹⁰⁸ used a more sophisticated model that treated the full three-dimensional motion of the hydrogen quantum mechanically. The former calculations thus neglected a substantial contribution from bending rearrangements of the C–H and O–H bonds. Very different effective masses and frequencies for the hydrogen stretching modes also were used in the two studies. These problems are compounded by the above-mentioned issue of the validity of eq 42. In addition, even advanced harmonic treatments of the modes that do not participate in the hydrogen motions¹⁰⁸ may not adequately reflect the anharmonicity of the intramolecular surface.

Knapp et al.⁹¹ found that the rate of hydrogen transfer was slowed by several orders of magnitude in L546A and L754A mutants of soybean lipoxygenase. Based on fits of the activation energy and the kinetic isotope effects to the predictions of eqs 42–45, they attributed the reduction in the rate constant to increases in λ_{cl} from about 20 kcal/mol in the wild-type enzyme to 30 kcal/mol in the L546A mutant and 36 kcal/mol in L754A. They ascribed these changes entirely to the environment ($\lambda_{\text{cl,out}}$). It appears to us that $\lambda_{\text{cl,out}}$ is unlikely to be larger than 2–3 kcal/mol in either the wild-type or the mutant enzyme, since the change in charge distribution during the reaction is small and calculated values of $\lambda_{\text{cl,out}}$ are similar in water and the protein.⁷⁹

In view of the difficulties in using the diabatic approximation for proton transfer, one would like to have a description that also is valid in the adiabatic limit. We have used the centroid path-integral strategy in a version called “quantized classical path” (QCP).^{114,115} This approach involves replacing a classical solute atom of mass m by a ring of p (on the order of 20) “quasiparticles.” The quasiparticles move on the effective potential

$$U_{\text{qm}} = \sum_{k=1}^p \frac{1}{2} mp(k_B T/\hbar)^2 |\Delta \vec{R}_k|^2 + \frac{1}{p} U(\vec{R}_k) \quad (46)$$

where \vec{R}_k is the position of the particle, $U(\vec{R}_k)$ is the potential used in a classical MD simulation, and $\Delta \vec{R}_k = \vec{R}_{k+1} - \vec{R}_k$ ($\vec{R}_{p+1} = \vec{R}_1$). The distribution of the quasiparticles, averaged over multiple simulations, represents the probability of finding the atom at various positions. The effective potential allows particles near the classical energy minimum to spread out and thus to have higher energy than a classical atom at the minimum, representing the zero-point energy. At the same time, a quasiparticle has a possibility of tunneling through regions where U_{qm} exceeds the classical energy, because U is divided by p .

Given the potential surface U_{qm} described by eq 46, the quantum mechanical activation free energy ($\Delta g_{\text{q}}^\ddagger$) can be evaluated and incorporated into the expression

$$k_q = \frac{\kappa_q k_B T}{h} \exp(-\Delta g_q^\ddagger / (k_B T)) \quad (47)$$

for the rate constant.^{116,117} The factor κ_q here is the quantum mechanical transmission coefficient, which as discussed above is usually close to unity.

Other treatments that are reliable for adiabatic processes are the MDQT (“molecular dynamics with quantum transitions”) method developed by Hammes-Schiffer and co-workers³¹ and the VTST (“variational transition state theory”) approach of Truhlar and co-workers.¹¹⁸ The MDQT method is a surface-hopping approach that is in spirit similar to eq 42 but is not limited to diabatic states. The VTST method is based on a consistent evaluation of the nuclear quantum mechanical correction by integrating the transition probability over different energy values. Like the QCP treatment, these methods allow one to include the protein motions in the classical region and thus provide a fully microscopic way of exploring vibrationally assisted nuclear tunneling. The inclusion of the protein fluctuations is less straightforward in the VTST approach than in the MDQT and QCP methods, although some progress has been made and the calculations nicely reproduce observed kinetic isotope effects.^{31,118}

As we have argued above, the question at issue is not whether nuclear quantum mechanical effects such as tunneling occur in some enzymatic reactions (they surely do), but whether these effects are significantly different in enzymes and solution.¹¹⁵ Although it is possible to address this question experimentally in some cases,^{119,120} it often is hard to perform experiments on the relevant reference reaction in solution. Computer simulations provide a natural way of comparing the two reactions. The results of QCP simulations for several types of enzyme and the corresponding solution reactions are collected in Table 1. In all the cases we have studied to date, including one that exhibits exceptionally large kinetic isotope effects (soybean lipoxygenase), we have obtained similar effects in enzymes and solutions. This seems to indicate that nuclear quantum mechanical effects do not provide a major catalytic factor. As shown in Table 2, the computer simulations are able to reproduce the activation free energies well, even when the contributions from tunneling are large. The importance of tunneling in the reaction catalyzed by lipoxygenase appears to result from the sharpness of the energy barrier in this reaction, which is not very different in the enzyme than in solution. The enzyme reduces the height of the barrier, but evidently has relatively little control over the width.⁷⁹

The activation free energies for lipoxygenase given in Table 2 ($\Delta g_{q(H)}^\ddagger$ and $\Delta g_{q(D)}^\ddagger$) are larger than some of the values of Δg_{00}^\ddagger that have been obtained by fitting the measured rate constants and isotope effects to eqs 42–45.¹⁰⁸ This potentially confusing difference results mainly from the fact that the activation free energy, $\Delta g_{mm'}^\ddagger$, in eq 44, does not include stretching of the carbon–proton bond that is broken in the reaction; $\Delta g_{mm'}^\ddagger$ thus is not the overall free-energy barrier for the reaction, which of course must include the effects of the hydrogen stretching coordinate. In eqs 42–45, the vibrational overlap integrals that allow tunneling are collected separately and put in the preexponential factor of the expression for the rate constant. In the QCP formulation (eqs 46 and 47), the tunneling correction to the rate constant is included in the activation free energy, which expresses the probability of finding the system at the TS. Although

Table 1. Observed and Calculated Primary Deuterium Kinetic Isotope Effects^a

enzyme	obsd ^a	ref ^a	calcd ^b (enzyme)	calcd ^b (water)	ref ^b
lactate dehydrogenase	2–3	(183)	5.0	5.6	(78)
carbonic anhydrase	3.8	(184)	2.3		(186)
	3.8	(185)	3.9		(115)
glyoxalase	3.0	(187)	5.0	3.6	(188)
alcohol dehydrogenase ^c	3.8	(189)			(1)
lipoxygenase	81	(91)	81	100	(79)

^a Experimentally measured ratio of k_{cat} in H₂O and D₂O (k_H/k_D). ^b Computer simulations using the QCP method ($k_{q(H)}/k_{q(D)}$). ^c In the case of alcohol dehydrogenase, Villà and Warshel¹ calculated only the total nuclear quantum mechanical contribution to the hydrogen transfer. They found it to be similar in the enzyme and water reactions, indicating that the kinetic isotope effect probably is similar in the two systems.

Table 2. Calculated and Observed Kinetic Parameters for Soybean Lipoxygenase^a

T (K)	$k_{q(H)}$ (s ⁻¹)	$k_{q(D)}$ (s ⁻¹)	KIE ^b	$\Delta g_{q(H)}^\ddagger$ (kcal/mol)	$\Delta g_{q(D)}^\ddagger$ (kcal/mol)
270	322 (189)	1.0 (2.0)	322 (95)	12.70 (13.02)	15.89 (15.47)
300	507 (297)	6.0 (3.7)	85 (80)	13.84 (14.16)	16.50 (16.79)
333	541 (392)	18 (5.7)	30 (69)	15.27 (15.46)	17.98 (18.67)

^a From Olsson et al.⁷⁹ The calculated values were obtained by the QCP method (eqs 46 and 47). Experimental data from Knapp et al.⁹¹ are given in parentheses. ^b Primary kinetic isotope effect ($k_{q(H)}/k_{q(D)}$).

the distinction is partly just a matter of perspective, Voth et al.^{117,121,122} have shown by path integral calculations that, if the preexponential factor in the TST rate equation is taken to be $\kappa_q k_B T/h$ as in eq 47, all the other factors that affect the rate can be incorporated rigorously in Δg_q^\ddagger .

11. Concerted Motions in an Enzyme Usually Do Not Make Dynamical Contributions to Catalysis

Nuclear magnetic resonance spectroscopy has been used to study the motions of enzymes over a wide range of time scales.^{22,123–126} An interesting case is the enzyme cyclophilin A, which catalyzes cis–trans isomerization of peptidyl proline bonds.^{22,123,127,128} A detailed analysis of the relaxation dynamics indicated that numerous residues of the protein have motions in the millisecond time range, coinciding with the turnover time of the enzyme and that some of these motions change when substrate is added. In particular, the transverse ¹⁵N amide relaxation of Arg 55, a residue that is hydrogen bonded to the substrate and is essential for catalysis, accelerates in the presence of the substrate and approximately matches the dynamics of forming the TS, suggesting that motions of Arg 55 might play a dynamical role in the catalytic mechanism.²² In analyzing this proposal, it is important to bear in mind that, if Arg 55 or any other residue moves along the reaction coordinate and if its position changes in the TS, it necessarily moves on the same time scale as the reaction. The solvent molecules in a reaction in solution, for example, must rearrange during the reaction and so must move at more or less the same rate as the solute atoms (see Figure 6). Most of the reorganization of the environment occurs on the same time scale as the reaction, and the motions of protein residues near the reacting substrate are not fundamentally different in this regard from the motions of the solvent molecules in solution. Further, as long

as the motions of the protein residues follow Boltzmann's law, they simply reflect probabilistic effects and not bona fide dynamical effects. In a QM/MM study of cyclophilin A, Li and Cui¹²⁸ found that Arg 55 underwent only very small displacements between the enzyme–substrate complex and the TS. They concluded that the arginine residue stabilizes the TS electrostatically and that its motions do not contribute significantly to the catalysis. In another interesting NMR study, Wolf-Watz et al.¹²⁹ recently found that the opening of a lid over the nucleotide-binding pocket limits the enzymatic reaction rates in homologues of adenylate kinase from both mesophilic and hyperthermophilic organisms, suggesting a close link between dynamics and catalysis. As pointed out in a commentary by Akke,¹³⁰ this was an exceptional study because, although lid movements have been described previously in numerous enzymes, Wolf-Watz et al. were able to measure the protein dynamics and the reaction kinetics under essentially identical conditions. It would, nevertheless, be unwarranted to conclude that the enzyme dynamics contributes importantly to catalysis. As discussed in section 2, catalysis is defined by the difference between the reaction rates in the enzyme and a reference reaction, and contributions to catalysis must be assessed according to this definition. The thermophilic and mesophilic enzymes both provide an enormous rate enhancement relative to the solution reaction, and the lid opening probably contributes little to this enhancement. Conformational changes such as lid opening or closing usually become rate-limiting only if the enzyme has reduced the activation barrier for the chemical step drastically by other mechanisms. Although the work of Wolf-Watz et al.¹²⁹ establishes a correlation between conformational changes and kinetics, this does not demonstrate a connection between dynamics and catalysis.

Wolf-Watz et al.¹²⁹ also address the general observation that thermophilic enzymes are slower than their mesophilic homologues at moderate temperatures. They conclude that the lower reaction rate in the hyperthermophilic adenylate kinase at ambient temperatures is caused solely by a lower rate of lid opening. This seems in line with the fact that the thermophilic homologue usually is more stable, although the barriers for local unfolding are not necessarily higher throughout the molecule and in some cases may be lower.^{129,130} Greater stability clearly does not imply that a thermophilic enzyme will stabilize the transition state for the chemical step more strongly than its mesophilic counterpart. In general, a more stable protein is likely to be less effective as a catalyst, since more of the preorganization needed for catalysis is invested in folding energy.¹³¹

Nunez et al.¹³² recently suggested that the catalytic reaction of purine nucleoside phosphorylase involves protein modes that reduce the barrier height by 20% by compressing the reacting fragments. To evaluate the contribution of such modes to catalysis, one must calculate the barrier height from the minimum in the ground state, taking into account the energy associated with the compression. Without such an analysis, it might appear that a sufficiently strong compression would eliminate the barrier completely. In addition, it is important to bear in mind that compression modes similar to those that occur in the protein also occur in the reference solution reaction. In the cases that we have studied, the costs of bringing the reactants to the same distance are similar in solution and in the enzyme, which means that the compression does not contribute significantly to catalysis (see the

related discussion of near-attack conformations in section 12).

Benkovic, Wright, and co-workers^{12,133–136} have studied the reaction of dihydrofolate reductase by NMR. They found that site-directed mutations of residues in a loop that undergoes relatively large backbone motions had detrimental effects on catalysis, and they suggested that the dynamics of these residues could be important for catalysis. This suggestion was supported by Brooks and co-workers,^{17,137} who carried out MD simulations of three ternary complexes of the enzyme. Motions of some residues were strongly correlated and were different in the enzyme–substrate and enzyme–product complexes. Some of these motions were modified in simulations of mutant enzymes with diminished activity. However, these studies did not examine any of the transition states in the reaction or demonstrate any dynamical effects on the rate constant. The different motions of the ES and EP complexes could just reflect the coupling between the enzyme–substrate interactions and interactions of various groups in the protein, which is common to all enzymes. In simulations using the MDQT approach, Hammes-Schiffer and co-workers^{137–139} identified a network of correlated conformational changes with projections on the reaction path but concluded that these reflect equilibrium structural effects rather than dynamical effects. QM/MM simulations described by Garcia-Vilcoia et al.¹⁴⁰ also appear to be in accord with this view.

It is important to emphasize that identification of correlated motions does not provide a new view of enzyme catalysis, because reorganization of the solvent along the reaction path in solution also involves highly correlated motions.^{28,78} Correlated motions of an enzyme do not necessarily contribute to catalysis and indeed could be detrimental if they increase the reorganization energy of the reaction. The EVB and dispersed-polaron approaches described above consider the enzyme reorganization explicitly and automatically assess the complete structural changes along the reaction coordinates. A dispersed-polaron analysis of the type presented in Figure 10, for example, tells us the projection of the protein motion on the reaction coordinate and provides a basis for a quantitative comparison with a reference reaction in solution.

Mutations of residues at considerable distances from the active site sometimes alter enzyme activities, and these effects could, in principle, reflect perturbations of global motions of the protein. In most cases, they more likely reflect long-range effects on ΔG^\ddagger . Such long-range coupling of free-energy changes has been seen in computer simulations of allosteric effects in hemoglobin¹⁴¹ and the effects of GTPase-activating proteins on the activity of p21^{ras}.¹⁴² Miller et al.¹⁴³ have described an impressive experimental demonstration of such an effect in orotidine 5'-phosphate decarboxylase, where removing the ribose 5'-phosphate moiety of the substrate decreases k_{cat}/K_m by more than 12 orders of magnitude.

Berendsen, Go, and their co-workers have identified collective motions in proteins by a method called "essential dynamics", in which they examine the covariance of positional fluctuations of the C_α atoms.^{15,144–146} They suggest that low-frequency global vibrational modes extracted by diagonalizing the covariance matrix have special functional significance. In proteins with several domains, these modes can reflect movements of one domain relative to another, and they sometimes correlate with structural variations between X-ray structures determined under different condi-

tions.¹⁴⁷ However, such fluctuations between different conformations do not necessarily have any functional importance: they could just reflect a relatively flat free energy surface along a particular coordinate. The significance of a protein motion depends on how the motion affects Δg^\ddagger for the process the enzyme catalyzes: motions that have little influence on Δg^\ddagger are unlikely to be of special significance.

The coupling of protein motions to a reaction in an enzyme involves fluctuating electrostatic interactions of the solute with charged or polar residues and bound water molecules. In solution, it involves reorientation of the solvation shells. Clearly, the reaction coordinate in both cases will involve components along the environment (solvent) coordinate. The real difference is the amplitude of the change in the solvent coordinates during the reaction, which determines the reorganization energy and generally is smaller in the enzyme because of preorganization of the active site.

12. Other Proposals for How Enzymes Work

This review has focused on whether dynamical effects contribute significantly to enzyme catalysis. If dynamical effects do not account for the catalytic power of enzymes, it is reasonable to ask what other factors are responsible for this power. Although this issue has been discussed extensively elsewhere,^{2,5,30,35,148} it may be helpful to summarize our perspective on the results of computer modeling of the main proposals.

(a) Electrostatic preorganization. The ability of enzymes to provide a preorganized electrostatic environment has been found to account for the major part of the catalytic effect in many enzymatic reactions.^{1,131,149,150} Other studies also have supported the view that electrostatic stabilization of the TS plays a major role in catalysis,^{35,151} although the importance of preorganization of the active site was not discussed.

(b) Steric strain. The idea that enzyme catalysis results from destabilization of the ground state was put forward in classical studies of lysozyme.¹⁵² Later studies that examined the actual amount of energy associated with steric strain found it to be small, due to the inherent flexibility of proteins.^{5,34,153} Nevertheless, the strain proposal has been invoked in several recent studies.^{154,155}

(c) Near-attack conformations (NAC). Bruice and co-workers have advanced the idea that enzymes catalyze reactions by favoring configurations in which the reactants are pushed to a close interaction distance.¹⁵⁶ In the cases we have studied, the energy associated with moving the reacting fragments from their average configuration in water to the average configuration in the enzymes was small, indicating that the corresponding catalytic effect was relatively minor.^{157,158} In one case where the NAC effect appeared to be large, it was found that the actual catalytic effect was attributable to electrostatic stabilization of the TS.¹⁵⁹ In other words, the NAC effect evidently was a consequence rather than the source of the electrostatic catalytic effect.¹⁵⁹

(d) Entropic effects. The idea that a loss of entropy upon substrate binding decreases the activation entropy for the rate-limiting catalytic step was advanced in the early work of Jencks and co-workers^{160,161} and has gained some support in recent computational studies.^{162,163} Villa et al. have argued that this proposal is based on an incomplete thermodynamic cycle.¹⁶⁴ The entropic contribution probably cannot be large since the activation entropy in solution is usually relatively small. This reflects the fact that the formation of the TS does not require losing many degrees of freedom.²⁹ Problems with

the entropy proposal also have emerged from experimental studies of cytidine deaminase by Wolfenden and co-workers.¹⁶⁵

(e) Desolvation. The idea that enzymes reduce the activation barrier by desolvating and destabilizing the ground state of the reacting fragments has been put forward by many workers.^{160,166–168} However, systematic analyses have shown that the TS is solvated much more strongly in many enzymes than in solution.^{2,5,61} The only way to test the desolvation proposal computationally is to calculate the actual binding energies of the reactants in the ground and transition states. This was done in the studies of haloalkane dehalogenase described above⁶¹ but not in most of the computational studies that have purported to favor desolvation effects.

(f) Low-barrier hydrogen bonds (LBHB). Some enzymes have been proposed to catalyze their reactions by forming so-called low-barrier hydrogen bonds (LBHB's) with the reactants.^{169–172} The distinction between this suggestion and the idea that preorganized hydrogen bonds stabilize the TS electrostatically¹³¹ is that a LBHB is a partially covalent (delocalized) bond, such as a bond of the form $Y^{\delta-}\cdots H\cdots X^{\delta-}$. Here Y is an enzyme atom and X could be, for example, an oxygen atom of the solute that becomes negatively charged in the TS. In our view, the gas-phase calculations that have been used to support the LBHB proposal have little relevance to enzymes. EVB studies and molecular orbital QM/MM studies that have reached a sufficiently quantitative level have failed to support the LBHB idea.^{173–176} Indeed, Warshel and Papazyan¹⁷⁷ showed that a LBHB would reduce rather than increase the solvation of the TS and thus would have an anticatalytic effect. Enzymes appear to stabilize the TS more effectively with localized charges than with delocalized charges.¹⁷⁷

In principle, enzymes could catalyze their reactions in many different ways, and it seems reasonable to assume that evolution has exploited all of these ways. However, the computer simulations and conceptual arguments summarized above indicate that most of the mechanisms that have been proposed do not lead to significant catalytic effects. These findings obviously cannot be extrapolated to enzymes that have not yet been studied. But the only way to examine the feasibility of a proposed effect is to assess its magnitude in a variety of known enzymes, and the finding that a particular effect is relatively unimportant in all these test cases raises the reasonable presumption that this effect cannot contribute significantly to catalysis.

Studies of catalytic antibodies have played a prominent role in the realization that enzymes stabilize transition states, since the antibodies were raised against haptens that were considered to be TS analogues.^{178–181} But, because the catalytic power of such antibodies is usually much smaller than that of natural enzymes, some workers have concluded that TS stabilization cannot account for the full catalytic power of enzymes, and it has been suggested that antibodies have less dynamical power than enzymes.²⁵ In one of the few computational studies that have addressed this point, the charge distribution in the TS of the reaction catalyzed by chorismate mutase was found to be quite different from the charge distribution in the TS analogue that was used to elicit a catalytic antibody for the same reaction.¹⁸² In many cases, it is not surprising that the catalytic antibody would be less effective than the enzyme, since the enzymatic reaction involves several transition states with similar energies and a

single hapten cannot mimic the charge distribution in more than one of these states.

13. Conclusions

From the discussion above, we conclude that there is no convincing evidence for dynamical contributions to enzyme catalysis of ground-state reactions. Although enzymes have evolved to lower the activation free energies of reactions dramatically, no enzyme has been shown to increase the transmission factor by more than a factor of about two relative to that for the same reaction in water. And although nuclear tunneling contributes to the reactions catalyzed by some enzymes, no enzyme has been shown to use a particular vibrational mode in a way that specifically enhances tunneling relative to the reaction in solution. Concerted, large-scale motions certainly occur in some enzymes, and like more localized motions of residues in the active site, these may correspond to motions that progress along the path to the TS. However, the rate constant is determined by the probability of reaching the TS rather than by the time dependence of fluctuations along the reaction path.

Of course we cannot say that an enzyme that exploits a dynamical effect will never be found. The search for dynamical effects undoubtedly will continue, generating additional intriguing results and providing an active meeting ground for investigators with new experimental and computational approaches. Our thesis is simply that to demonstrate a dynamical effect, one must show that it contributes significantly to catalysis in the enzyme and does not occur in the same reaction in solution.

14. Acknowledgment

This work was supported by NIH Grants GM24492 and GM40283 and NSF Grant MCB-0342276 to A.W. and NSF Grant MCB-9904618 to W.P. We gratefully acknowledge the University of Southern California's High Performance Computing and Communications Center for computer time.

15. References

- Villà, J.; Warshel, A. *J. Phys. Chem. B* **2001**, *105*, 7887.
- Shurki, A.; Warshel, A. *Adv. Protein Chem.* **2003**, *66*, 249.
- Leatherbarrow, R. J.; Fersht, A. R.; Winter, G. *Proc. Natl. Acad. Sci. U.S.A.* **1985**, *82*, 7840.
- Roca, M.; Marti, S.; Andres, J.; Moliner, V.; Tunon, M.; Bertran, J.; Williams, A. H. *J. Am. Chem. Soc.* **2003**, *125*, 7726.
- Warshel, A. *Computer Modeling of Chemical Reactions in Enzymes and Solutions*; John Wiley & Sons: New York, 1997.
- Karplus, M.; McCammon, J. A. *Annu. Rev. Biochem.* **1983**, *53*, 263.
- Neria, E.; Karplus, M. *Chem. Phys. Lett.* **1997**, *267*, 23.
- Careri, G.; Fasella, P.; Gratton, E. *Annu. Rev. Biophys. Bioeng.* **1979**, *8*, 69.
- Gavish, B.; Werber, M. M. *Biochemistry* **1979**, *18*, 1269.
- McCammon, J. A.; Wolynes, P. G.; Karplus, M. *Biochemistry* **1979**, *18*, 927.
- Cannon, W. R.; Singleton, S. F.; Benkovic, S. J. *Nat. Struct. Biol.* **1996**, *3*, 821.
- Miller, G. P.; Benkovic, S. J. *Biochemistry* **1998**, *37*, 6327.
- Zavodszky, P.; Kardos, J.; Svingor, A.; Petsko, G. A. *Proc. Natl. Acad. Sci. U.S.A.* **1998**, *95*, 7406.
- Kohen, A.; Klinman, J. P. *Chem. Biol.* **1999**, *6*, R191.
- Berendsen, H. J. C.; Hayward, S. *Curr. Opin. Struct. Biol.* **2000**, *10*, 165.
- Northrop, D. B.; Cho, Y. K. *Biochemistry* **2000**, *39*, 2406.
- Radkiewicz, J. L.; Brooks, C. L. *J. Am. Chem. Soc.* **2000**, *122*, 225.
- Kohen, A.; Cannio, R.; Bartolucci, S.; Klinman, J. P. *Nature* **1999**, *399*, 496.
- Daniel, R. M.; Dunn, R. V.; Finney, J. L.; Smith, J. C. *Annu. Rev. Biophys. Biomol. Struct.* **2003**, *32*, 69.
- Xie, X. S.; Lu, H. P. *J. Biol. Chem.* **1999**, *274*, 15967.
- Wilson, E. K. *Chem. Eng. News* **2000**, *78*, 42.
- Eisenmesser, E. Z.; Bosco, D. A.; Akke, M.; Kern, D. *Science* **2002**, *295*, 1520.
- Nam, K.; Prat-Resina, X.; Garcia-Viloca, M.; Devi-Kesavan, L. S.; Gao, J. L. *J. Am. Chem. Soc.* **2004**, *126*, 1369.
- Antoniou, D.; Schwartz, S. D. *Proc. Natl. Acad. Sci. U.S.A.* **1997**, *94*, 12360.
- Basran, J.; Sutcliffe, M. J.; Scrutton, N. S. *Biochemistry* **1999**, *38*, 3218.
- Bruno, W.; Bialek, W. *Biophys. J.* **1992**, *63*, 689.
- Liang, X.-Z.; Klinman, J. P. *Curr. Opin. Struct. Biol.* **2004**, *14*, 648.
- Warshel, A. *Proc. Natl. Acad. Sci. U.S.A.* **1984**, *81*, 444.
- Warshel, A.; Sussman, F.; Hwang, J. K. *J. Mol. Biol.* **1988**, *201*, 139.
- Warshel, A.; Parson, W. W. *Q. Rev. Biophys.* **2001**, *34*, 563.
- Billeter, S. R.; Webb, S. P.; Agarwal, P. K.; Iordanov, T.; Hammes-Schiffer, S. *J. Am. Chem. Soc.* **2001**, *123*, 11262.
- Thorpe, I. F.; Brooks, C. L., III. *J. Phys. Chem. B* **2003**, ASAP.
- Wolfenden, R.; Snider, M. J. *Acc. Chem. Res.* **2001**, *34*, 938.
- Warshel, A.; Levitt, M. *J. Mol. Biol.* **1976**, *103*, 227.
- Field, M. J. *J. Comput. Chem.* **2002**, *23*, 48.
- Olsson, M. H. M.; Hong, G.; Warshel, A. *J. Am. Chem. Soc.* **2003**, *125*, 5025.
- Strajbl, M.; Hong, G. Y.; Warshel, A. *J. Phys. Chem. B* **2002**, *106*, 13333.
- Zhang, Y. K.; Liu, H. Y.; Yang, W. T. *J. Chem. Phys.* **2000**, *112*, 3483.
- Warshel, A.; Weiss, R. M. *J. Am. Chem. Soc.* **1980**, *102*, 6218.
- Hwang, J. K.; King, G.; Creighton, S.; Warshel, A. *J. Am. Chem. Soc.* **1988**, *110*, 5297.
- Warshel, A.; Chu, Z. T.; Hwang, J. K. *Chem. Phys.* **1991**, *158*, 303.
- Hwang, J. K.; Creighton, S.; King, G.; Whitney, D.; Warshel, A. *J. Chem. Phys.* **1988**, *89*, 859.
- Marcus, R. A. *Annu. Rev. Phys. Chem.* **1964**, *15*, 155.
- Marcus, R. A. *Angew. Chem., Int. Ed. Engl.* **1993**, *32*, 1111.
- Keck, J. C. *Adv. Chem. Phys.* **1966**, *13*, 85.
- Bennett, C. H. In *Algorithms for chemical computations*; Christoferson, R. E., Ed.; American Chemical Society: Washington, DC, 1977.
- Chandler, D. *J. Chem. Phys.* **1978**, *68*, 2959.
- Montgomery, J. A.; Chandler, D.; Berne, B. J. *J. Chem. Phys.* **1979**, *70*, 4056.
- Grimmelmann, E. K.; Tully, J. C.; Helfand, E. *J. Chem. Phys.* **1981**, *74*, 5300.
- Straub, J. E.; Berne, B. J. *J. Chem. Phys.* **1985**, *83*, 1138.
- Cline, R. E.; Wolynes, P. G. *J. Chem. Phys.* **1987**, *86*, 3836.
- Anderson, J. B. *J. Chem. Phys.* **1973**, *58*, 4684.
- Rosenberg, R. O.; Berne, B. J.; Chandler, D. *Chem. Phys. Lett.* **1980**, *75*, 162.
- Anderson, J. B. *Adv. Chem. Phys.* **1995**, *91*, 381.
- Kubo, R. *Rep. Prog. Phys.* **1966**, *29*, 255.
- Warshel, A.; Hwang, J. K. *J. Chem. Phys.* **1986**, *84*, 4938.
- Maroncelli, M.; Fleming, G. R. *J. Chem. Phys.* **1988**, *89*, 5044.
- Fleming, G. R.; Wolynes, P. G. *Phys. Today* **1990**, *43*, 36.
- Nandi, N.; Bhattacharyya, K.; Bagchi, B. *Chem. Rev.* **2000**, *100*, 2013.
- Pal, S. K.; Peon, J.; Zewail, A. H. *Proc. Natl. Acad. Sci. U.S.A.* **2002**, *99*, 15297.
- Olsson, M. H. M.; Warshel, A. *J. Am. Chem. Soc.* **2004**, *126*, 15167.
- Parson, W. W.; Warshel, A. *J. Phys. Chem. B* **2004**, *108*, 10474.
- Kurz, J. L.; Kurz, L. C. *Isr. J. Chem.* **1985**, *26*, 339.
- Warshel, A.; Bentzien, J. In *Transition State Modeling for Catalysis*; Truhlar, D. G., Morokuma, K., Eds.; ACS Symposium Series 721; American Chemical Society: Washington, DC, 1999.
- Cui, Q.; Karplus, M. *J. Am. Chem. Soc.* **2002**, *124*, 3093.
- Cui, Q. A.; Karplus, M. *J. Phys. Chem. B* **2002**, *106*, 7927.
- Bergsma, J. P.; Gertner, B. J.; Wilson, K. R.; Hynes, J. T. *J. Chem. Phys.* **1987**, *86*, 1356.
- Gertner, B. J.; Wilson, K. R.; Hynes, J. T. *J. Chem. Phys.* **1989**, *90*, 3537.
- Truhlar, D. G.; Schenter, G. K.; Garret, B. C. *J. Chem. Phys.* **1993**, *98*, 5756.
- Muller, R. P.; Warshel, A. *J. Phys. Chem.* **1995**, *99*, 17516.
- Garcia-Viloca, M.; Gao, J.; Karplus, M.; Truhlar, D. G. *Science* **2004**, *303*, 186.
- Warshel, A.; Parson, W. W. *Q. Rev. Biophys.* **2001**, *34*, 563.
- Bentzien, J.; Muller, R. P.; Florian, J.; Warshel, A. *J. Phys. Chem. B* **1998**, *102*, 2293.
- Gertner, B. J.; Bergsma, J. P.; Wilson, K. R.; Lee, S. Y.; Hynes, J. T. *J. Chem. Phys.* **1987**, *86*, 1377.
- Neria, E.; Karplus, M. *J. Chem. Phys.* **1996**, *105*, 10812.
- Gertner, B. J.; Wilson, K. R.; Hynes, J. T. *J. Chem. Phys.* **1989**, *90*, 3537.

- (77) Cannon, W. R.; Singleton, S. F.; Benkovic, S. J. *Nat. Struct. Biol.* **1996**, *3*, 821.
- (78) Hwang, J. K.; Chu, Z. T.; Yadav, A.; Warshel, A. *J. Phys. Chem.* **1991**, *95*, 8445.
- (79) Olsson, M. H. M.; Siegbahn, P. E. M.; Warshel, A. *J. Am. Chem. Soc.* **2004**, *126*, 2820.
- (80) Basu, G.; Kitao, A.; Kuki, A.; Go, N. *J. Phys. Chem. B* **1998**, *102*, 2076.
- (81) Åqvist, J.; Fothergill, M. *J. Biol. Chem.* **1996**, *271*, 10010.
- (82) Warshel, A.; Chu, Z. T. *J. Chem. Phys.* **1990**, *93*, 4003.
- (83) Warshel, A. *J. Phys. Chem.* **1982**, *86*, 2218.
- (84) Borgis, D.; Lee, S.; Hynes, J. T. *Chem. Phys. Lett.* **1989**, *162*, 19.
- (85) Borgis, D.; Hynes, J. T. *J. Phys. Chem.* **1996**, *100*, 1118.
- (86) Parson, W. W.; Warshel, A. *Chem. Phys.* **2004**, *296*, 201.
- (87) Vos, M. H.; Lambry, J. C.; Robles, S. J.; Youvan, D. C.; Breton, J.; Martin, J. L. *Proc. Natl. Acad. Sci. U.S.A.* **1991**, *88*, 8885.
- (88) Vos, M. H.; Rischel, C.; Jones, M. R.; Martin, J. L. *Biochemistry* **2000**, *39*, 8353.
- (89) Yakovlev, A. G.; Shkuropatov, A. C.; Shuvalov, A. V. *FEBS Lett.* **2000**, *466*, 209.
- (90) Carpenter, B. K. *J. Phys. Org. Chem.* **2003**, *16*, 858.
- (91) Knapp, M. J.; Rickert, K.; Klinman, J. P. *J. Am. Chem. Soc.* **2002**, *124*, 3865.
- (92) Haffa, A. L. M.; Lin, S.; Katilius, E.; Williams, J. C.; Taguchi, A. K. W.; Allen, J. P.; Woodbury, N. W. *J. Phys. Chem. B* **2002**, *106*, 7376.
- (93) Swain, C. G.; Stivers, E. C.; Reuwer, J. F.; Schaad, L. J. *J. Am. Chem. Soc.* **1958**, *80*, 5885.
- (94) Saunders, W. H. *J. Am. Chem. Soc.* **1985**, *107*, 164.
- (95) Kohen, A.; Klinman, J. P. *Acc. Chem. Res.* **1998**, *31*, 397.
- (96) Bahnsen, B. J.; Colby, T. D.; Chin, J. K.; Goldstein, B. M.; Klinman, J. P. *Proc. Natl. Acad. Sci. U.S.A.* **1997**, *94*, 12797.
- (97) Tsai, S.-C.; Klinman, J. P. *J. Am. Chem. Soc.* **2001**, *123*, 2303.
- (98) Grant, K. L.; Klinman, J. P. *Biochemistry* **1989**, *28*, 6597.
- (99) Jonsson, T.; Glickman, M. H.; Sun, S. J.; Klinman, J. P. *J. Am. Chem. Soc.* **1996**, *118*, 10319.
- (100) Kohen, A.; Jonsson, T.; Klinman, J. P. *Biochemistry* **1997**, *36*, 6854.
- (101) Kohen, A.; Klinman, J. P. *J. Am. Chem. Soc.* **2000**, *122*, 10738.
- (102) Levy, R. M.; Gallicchio, E. *Annu. Rev. Phys. Chem.* **1998**, *49*, 531.
- (103) Villà, J.; Strajbl, M.; Glennon, T. M.; Sham, Y. Y.; Chu, Z. T.; Warshel, A. *Proc. Natl. Acad. Sci. U.S.A.* **2000**, *97*, 11899–11904.
- (104) Rickert, K. W.; Klinman, J. P. *Biochemistry* **1999**, *38*, 12218.
- (105) Knapp, M. J.; Klinman, J. P. *Eur. J. Biochem.* **2002**, *269*, 3113.
- (106) Lewis, E. R.; Johansen, E.; Holman, T. R. *J. Am. Chem. Soc.* **1999**, *121*, 1395.
- (107) Lehnert, N.; Solomon, E. I. *J. Biol. Inorg. Chem.* **2003**, *8*, 294.
- (108) Hatcher, E.; Soudackov, A. V.; Hammes-Schiffer, S. *J. Am. Chem. Soc.* **2004**, *126*, 5763.
- (109) Cui, Q.; Elstner, M.; Karplus, M. *J. Phys. Chem. B* **2002**, *106*, 2721.
- (110) Kuznetsov, A. M.; Ulstrup, J. *Can. J. Chem.* **1999**, *77*, 1085.
- (111) Borgis, D.; Hynes, J. T. *J. Chem. Phys.* **1991**, *94*, 3619.
- (112) Ball, P. *Nature* **2004**, *431*, 396.
- (113) Muegge, I.; Qi, P. X.; Wand, A. J.; Chu, Z. T.; Warshel, A. *J. Phys. Chem. B* **1997**, *101*, 825.
- (114) Hwang, J. K.; Warshel, A. *J. Phys. Chem.* **1993**, *97*, 10053.
- (115) Hwang, J. K.; Warshel, A. *J. Am. Chem. Soc.* **1996**, *118*, 11745.
- (116) Gillan, M. J. *J. Phys. C: Solid State Phys.* **1987**, *20*, 3621.
- (117) Voth, G. A. *Adv. Chem. Phys.* **1996**, *93*, 135.
- (118) Gao, J. L.; Truhlar, D. G. *Annu. Rev. Phys. Chem.* **2002**, *53*, 467.
- (119) Kemsley, J. *Chem. Eng. News* **2003**, *81*, 29.
- (120) Doll, K. M.; Bender, B. R.; Finke, R. G. *J. Am. Chem. Soc.* **2003**, *125*, 10877.
- (121) Voth, G. A.; Chandler, D.; Miller, W. H. *J. Chem. Phys.* **1989**, *91*, 7749.
- (122) Voth, G. A. *J. Phys. Chem.* **1993**, *97*, 8365.
- (123) Akke, M. *Curr. Opin. Struct. Biol.* **2002**, *12*, 642.
- (124) Wang, L. C.; Pang, Y. X.; Holder, T.; Brender, J. R.; Kurochkin, A. V.; Zuiderweg, E. R. P. *Proc. Natl. Acad. Sci. U.S.A.* **2001**, *98*, 7684.
- (125) Palmer, A. G.; Kroenke, C. D.; Loria, J. P. *Nucl. Magn. Reson. Biol. Macromol., Part B* **2001**, *339*, 204.
- (126) Palmer, A. G. *Chem. Rev.* **2004**, *104*, 3623.
- (127) Falke, J. *J. Science* **2002**, *295*, 1480.
- (128) Li, G. H.; Cui, Q. *J. Am. Chem. Soc.* **2003**, *125*, 15028.
- (129) Wolf-Watz, M.; Thai, V.; Henzler-Wildman, K.; Hadjipavlou, G.; Eisenmesser, E. Z.; Kern, D. *Nat. Struct. Mol. Biol.* **2004**, *11*, 945.
- (130) Akke, M. *Nat. Struct. Mol. Biol.* **2004**, *11*, 912.
- (131) Warshel, A. *Proc. Natl. Acad. Sci. U.S.A.* **1978**, *75*, 5250.
- (132) Nunez, S.; Antoniou, D.; Schramm, V. L.; Schwartz, S. D. *J. Am. Chem. Soc.* **2004**, *126*, 15720.
- (133) Cameron, C. E.; Benkovic, S. J. *Biochemistry* **1997**, *36*, 15792.
- (134) Epstein, D. M.; Benkovic, S. J.; Wright, P. E. *Biochemistry* **1995**, *34*, 11037.
- (135) Schnell, J. R.; Dyson, H. J.; Wright, P. E. *Biochemistry* **2004**, *43*, 374.
- (136) Schnell, J. R.; Dyson, H. J.; Wright, P. E. *Annu. Rev. Biophys. Biomol. Struct.* **2004**, *33*, 119.
- (137) Rod, T. H.; Radkiewicz, J. L.; Brooks, C. L. *Proc. Natl. Acad. Sci. U.S.A.* **2003**, *100*, 6980.
- (138) Watney, J. B.; Agarwal, P. K.; Hammes-Schiffer, S. *J. Am. Chem. Soc.* **2003**, *125*, 3745.
- (139) Hammes-Schiffer, S. *Curr. Opin. Struct. Biol.* **2004**, 192.
- (140) Garcia-Viloca, M.; Truhlar, D. G.; Gao, J. L. *Biochemistry* **2003**, *42*, 13558.
- (141) Warshel, A.; Weiss, R. M. *J. Am. Chem. Soc.* **1981**, *103*, 446.
- (142) Glennon, T. M.; Villa, J.; Warshel, A. *Biochemistry* **2000**, *39*, 9641.
- (143) Miller, B.; Snider, M. J.; Short, S.; Wolfenden, R. *Biochemistry* **2000**, *39*, 8113.
- (144) Amadei, A.; Linssen, A. B. M.; Berendsen, H. J. C. *Proteins: Struct., Funct., Genet.* **1993**, *17*, 412.
- (145) Van Aalten, D. M. F.; De Groot, D. M. F.; Findlay, J. B. C.; Berendsen, H. J. C.; Amadei, A. *J. Comput. Chem.* **1997**, *18*, 169.
- (146) Kitao, A.; Go, N. *Curr. Opin. Struct. Biol.* **1999**, *9*, 164.
- (147) de Groot, B. L.; Hayward, S.; van Aalten, D. M. F.; Amadei, A.; Berendsen, H. J. C. *Proteins* **1998**, *31*, 116.
- (148) Marti, S.; Roca, M.; Andres, J.; Moliner, V.; Silla, E.; Tunon, I.; Bertran, J. *Chem. Soc. Rev.* **2004**, *33*, 98.
- (149) Rao, S. N.; Singh, U. C.; Bash, P. A.; Kollman, P. A. *Nature* **1987**, *328*, 551.
- (150) Feierberg, I.; Åqvist, J. *Biochemistry* **2002**, *41*, 15728.
- (151) Soman, K.; Yang, A. S.; Honig, B.; Fletterick, R. *Biochemistry* **1989**, *28*, 9918.
- (152) Blake, C. C. F.; Johnson, L. N.; Mair, G. A.; North, A. C. T.; Phillips, D. C.; Sarma, V. R. *Proc. R. Soc., Ser. B* **1967**, *167*, 378.
- (153) Levitt, M. In *Peptides, Polypeptides and Proteins*; Blout, E. R., Bovey, F. A., Goodman, M., Lotan, N., Eds.; John Wiley & son: New York, 1974.
- (154) Khanjin, N. A.; Snyder, J. P.; Menger, F. M. *J. Am. Chem. Soc.* **1999**, *121*, 11831.
- (155) Tapia, O.; Andres, J.; Safont, V. S. *J. Chem. Soc., Faraday Trans.* **1994**, *90*, 2365.
- (156) Hur, S.; Bruice, T. C. *J. Am. Chem. Soc.* **2003**, *125*, 1472.
- (157) Shurki, A.; Villa, J.; Warshel, A. *Abstr. Pap. Am. Chem. Soc.* **2002**, *223*, C59.
- (158) Ranaghan, K. E.; Mulholland, A. J. *Chem. Commun.* **2004**, 1238.
- (159) Strajbl, M.; Shurki, A.; Kato, M.; Warshel, A. *J. Am. Chem. Soc.* **2003**, *125*, 10228.
- (160) Jencks, W. P. *Catalysis in Chemistry and Enzymology*; Dover Publication: New York, 1986.
- (161) Page, M. I.; Jencks, W. P. *Proc. Natl. Acad. Sci. U.S.A.* **1971**, *68*, 1678.
- (162) Stanton, R. V.; Perakyla, M.; Bakowies, D.; Kollman, P. A. *J. Am. Chem. Soc.* **1998**, *120*, 3448.
- (163) Kollman, P. A.; Kuhn, B.; Donini, O.; Perakyla, M.; Stanton, R.; Bakowies, D. *Acc. Chem. Res.* **2001**, *34*, 72.
- (164) Villa, J.; Strajbl, M.; Glennon, T. M.; Sham, Y. Y.; Chu, Z. T.; Warshel, A. *Proc. Natl. Acad. Sci. U.S.A.* **2000**, *97*, 11899.
- (165) Snider, M. J.; Gaunitz, S.; Ridgway, C.; Short, S. A.; Wolfenden, R. *Biochemistry* **2000**, *39*, 9746.
- (166) Crosby, J.; Stone, R.; Lienhard, G. E. *J. Am. Chem. Soc.* **1970**, *92*, 2891.
- (167) Lee, J. K.; Houk, K. N. *Science* **1997**, *276*, 942.
- (168) Devi-Kesavan, L. S.; Gao, J. L. *J. Am. Chem. Soc.* **2003**, *125*, 1532.
- (169) Frey, P. A.; Whitt, S. A.; Tobin, J. B. *Science* **1994**, *264*, 1927.
- (170) Cleland, W. W.; Kreevoy, M. M. *Science* **1994**, *264*, 1887.
- (171) Pan, Y.; McAllister, M. A. *J. Am. Chem. Soc.* **1998**, *120*, 166.
- (172) Pan, Y.; McAllister, M. A. *J. Org. Chem.* **1997**, *62*, 8171.
- (173) Schutz, C. N.; Warshel, A. *J. Phys. Chem. B* **2004**, *108*, 2066.
- (174) Garcia-Viloca, M.; Gonzalez-Lafont, A.; Lluch, J. M. *J. Am. Chem. Soc.* **2001**, *123*, 709.
- (175) Molina, P. A.; Sikorski, R. S.; Jensen, J. H. *Theor. Chem. Acc.* **2003**, *109*, 100.
- (176) Mulholland, A. J.; Lyne, P. D.; Karplus, M. *J. Am. Chem. Soc.* **2000**, *122*, 534.
- (177) Warshel, A.; Papazyan, A. *Proc. Natl. Acad. Sci. U.S.A.* **1996**, *93*, 13665.
- (178) Pollack, S. J.; Jacobs, J. W.; Schultz, P. G. *Science* **1986**, *234*, 1570.
- (179) Trombantano, A.; Janda, K. D.; Lerner, R. A. *Science* **1986**, *234*, 1566.
- (180) Hilvert, D. *Annu. Rev. Biochem.* **2000**, *69*, 751.
- (181) Mader, M. M.; Bartlett, P. A. *Chem. Rev.* **1997**, *97*, 1281.
- (182) Barbany, M.; Gutierrez-de-Teran, H.; Sanz, F.; Villa-Freixa, J.; Warshel, A. *ChemBiochem* **2003**, *4*, 277.

- (183) Clarke, A. R.; Wilks, H. M.; Barstow, D. A.; Atkinson, T.; Chia, W. N.; Holbrook, J. J. *Biochemistry* **1988**, *27*, 1617.
- (184) Silverman, D. N.; Lindskog, S. *Acc. Chem. Res.* **1988**, *21*, 30.
- (185) Steiner, H.; Jonsson, B. H.; Lindskog, S. *Eur. J. Biochem.* **1975**, *14*, 253.
- (186) Warshel, A.; Hwang, J. K.; Aqvist, J. *Faraday Discuss.* **1992**, 225.
- (187) Ridderstrom, M.; Cameron, A. D.; Jones, T. A.; Mannervik, B. *Biochem. J.* **1997**, *328*, 231.
- (188) Feierberg, I.; Luzhkov, V.; Aqvist, J. *J. Biol. Chem.* **2000**, 275, 22657.
- (189) Bahnson, B. J.; Park, D. H.; Kim, K.; Plapp, B. V.; Klinman, J. P. *Biochemistry* **1993**, *32*, 5503.
- (190) Truhlar, D. G. In *Isotope Effects in Chemistry and Biology*; Kohen, A., Limach, H. H., Eds.; Taylor and Francis: Boca Raton, FL, 2006.

CR040427E